# Structural and functional insights into the candidate genes associated with different developmental stages of flag leaf in bread wheat (Triticum aestivum L.)

Sheetal Mehla[1], Dr Upendra Kumar[1*], Prexha Kapoor[1], Yogita Singh[1], Pooja Sihag[1], Vijeta Sagwal[1], Priyanka Balyan[2], Anuj Kumar[3], Navjeet Ahalawat[1], Nita Lakra[1], Krishna Pal[4], Reyazul R. Mir[5], Om P. Dhankher[6]

[1]Department of Molecular Biology, Biotechnology & Bioinformatics, College of Basic Sciences and Humanities, Chaudhary Charan Singh Haryana Agricultural University, India, [2]Department of Botany, Deva Nagri, College, India, [3]Indian Agricultural Statistics Research Institute, Indian Council of Agricultural Research, India, [4]Biophysics Unit, College of Basic Sciences & Humanities, GB Pant University of Agriculture & Technology, Pantnagar, India., India, [5]Division of Genetics and Plant Breeding, Faculty of Agriculture, Sher-e-Kashmir University of Agricultural Sciences and Technology, India, [6]Stockbridge School of Agriculture, University of Massachusetts Amherst, United States



*Submitted to Journal:*
Frontiers in Genetics

*Specialty Section:*
Plant Genomics

*Article type:*
Original Research Article

*Manuscript ID:*
933560

*Received on:*
01 May 2022

*Revised on:*
09 Jun 2022

*Journal website link:*
www.frontiersin.org

## Conflict of interest statement

The authors declare that the research was conducted in the absence of any commercial or financial relationships that could be construed as a potential conflict of interest

## Author contribution statement

SM performed bioinformatics data analysis. NA performed molecular dynamics simulation of modelled structures. SM, PK, YS, PS and VS drafted the manuscript.


## Keywords

Flag leaf development, Homology Modeling, Gene expression analyses, qRT-PCR (quantitative real-time polymerase chain reaction), MD simulation



## Abstract

Word count: 245

Grain yield is one of the most important aims for combating the needs of the growing world population. The role of development and nutrient transfer in flag leaf for higher yields at the grain level is well known. It is a great challenge to properly exploit this knowledge because all the processes, starting from the emergence of the flag leaf to the grain filling stages of wheat (Triticum aestivum L.), are very complex biochemical and physiological processes to address. This study was conducted with the primary goal of functionally and structurally annotating the candidate genes associated with different developmental stages of flag leaf in a comprehensive manner using a plethora of in-silico tools. Flag leaf associated genes were analyzed for their structural and functional impact using a set of bioinformatics tools and algorithms. The results revealed the association of 17 candidate genes with different stages of flag leaf development in wheat crops. Of these 17 candidate genes, the expression analysis results revealed the upregulation of genes such as TaSRT1-5D, TaPNH1-7B, and TaNfl1-2B and the downregulation of genes such as TaNAP1-7B, TaNOL-4D and TaOsl2-2B can be utilized for the generation of high yielding wheat varieties. Through MD simulation and other in-silico analysis, all these proteins were found to be stable. Based on the outcome of bioinformatics and molecular analysis, the identified candidate genes were found to play a principal role in the flag leaf development process and can be utilized for higher yield production in wheat.


## Contribution to the field

Grain yield is one of the most important aims for combating the needs of the growing world population. The role of development and nutrition transfer of flag leaf for higher yields at the level of grain is well known to us. It's a great challenge to exploit this knowledge properly because all the processes, starting from the emergence of the flag leaf to the grain filling stages of wheat (Triticum aestivum L.), are very complex biochemical and physiological processes to deal with. This study was conducted with the primary goal of functionally and structurally annotating the candidate genes associated with different developmental stages of flag leaf in a comprehensive manner using a plethora of in-silico tools. Flag leaf associated genes were analyzed for their structural and functional impact using a set of bioinformatics tools and algorithms including EnsemblPlant, GSDS v2.0, Protparam, Swiss model server, UCSF ChimeraX, ProFunc, ProCheck, Genevestigator, GeneMANIA, STITCH server, GROMACS-2020 and MegaX.4. The results revealed the association of 17 candidate genes with different stages of flag leaf development in wheat crops. Of these 17 candidate genes expression analysis results revealed the upregulation of genes like TaSRT1-5D, TaPNH1-7B, and TaNfl1-2B and downregulating genes like TaNAP1-7B, TaNOL-4D, TaOsl2-2B can be utilized for the generation of high yielding wheat varieties. Through MD simulation and other in-silico analyses all these proteins were found stable. Based on the outcome of bioinformatics and molecular analysis, identified candidate genes were found to play a principal role in the flag leaf development process and can be utilized for higher yield production in wheat.

## *Ethics statements*

### *Studies involving animal subjects*
Generated Statement: No animal studies are presented in this manuscript.

### *Studies involving human subjects*
Generated Statement: No human studies are presented in this manuscript.

### *Inclusion of identifiable human data*
Generated Statement: No potentially identifiable human images or data is presented in this study.

## *Data availability statement*

Generated Statement: The original contributions presented in the study are included in the article/supplementary material, further inquiries can be directed to the corresponding author/s.

# Structural and functional insights into the candidate genes associated with different developmental stages of flag leaf in bread wheat (*Triticum aestivum* L.)

**Sheetal Mehla[1†], Upendra Kumar[1†*], Prexha Kapoor[1], Yogita Singh[1], Pooja Sihag[1], Vijeta Sagwal[1], Priyanka Balyan[2], Anuj Kumar[3], Navjeet Ahalawat[1], Nita Lakra[1], Krishna Pal Singh[4&5], Vladan Pesic[6], Ivica Djalovi[7], Reyazul Rouf Mir[8], Om Parkash Dhankher[9],**

[1*]Department of Molecular Biology, Biotechnology and Bioinformatics, College of Biotechnology, CCS Haryana Agricultural University, Hisar, 125004, India

[2]Department of Botany, Deva Nagri P.G. College, CCS University, Meerut-250001, India

[3]Shantou University Medical College, Shantou, PRC, Dalhousie University, Halifax, Nova, Scotia, Canada.

[4]Biophysics Unit, College of Basic Sciences & Humanities, GB Pant University of Agriculture & Technology, Pantnagar, 263145, India.

[5]Vice-Chancellor's Secretariat, Mahatma Jyotiba Phule Rohilkhand University, Bareilly-243001, India

[6]Department of Genetics and Plant Breeding, Faculty of Agriculture, University of Belgrade, Serbia

[7]Institute of Field and Vegetable Crops, National Institute of the Republic of Serbia, Maxim Gorki 30, 21000 Novi Sad, Serbia

[8]Division of Genetics and Plant Breeding, Sher-e-Kashmir University of Agricultural Sciences and Technology of Kashmir (SKUAST-Kashmir), Srinagar (J& K), India

[9]Stockbridge School of Agriculture, University of Massachusetts Amherst, MA, 01003, USA

[*]**Corresponding Authors:**

Dr. Upendra Kumar, Email: baliyan.upendra@gmail.com

[†]These authors have contributed equally to this work and share first authorship

# Abstract

Grain yield is one of the most important aims for combating the needs of the growing world population. The role of development and nutrient transfer in flag leaf for higher yields at the grain level is well known. It is a great challenge to properly exploit this knowledge because all the processes, starting from the emergence of the flag leaf to the grain filling stages of wheat (*Triticum aestivum* L.), are very complex biochemical and physiological processes to address. This study was conducted with the primary goal of functionally and structurally annotating the candidate genes associated with different developmental stages of flag leaf in a comprehensive manner using a plethora of *in-silico* tools. Flag leaf associated genes were analyzed for their structural and functional impact using a set of bioinformatics tools and algorithms. The results revealed the association of 17 candidate genes with different stages of flag leaf development in wheat crops. Of these 17 candidate genes, the expression analysis results revealed the upregulation of genes such as TaSRT1-5D, TaPNH1-7B, and TaNfl1-2B and the downregulation of genes such as TaNAP1-7B, TaNOL-4D and TaOsl2-2B can be utilized for the generation of high yielding wheat varieties. Through MD simulation and other *in-silico* analysis, all these proteins were found to be stable. Based on the outcome of bioinformatics and molecular analysis, the identified candidate genes were found to play a principal role in the flag leaf development process and can be utilized for higher yield production in wheat.



**Keywords:** Flag leaf development; *in-silico* analysis; expression analysis, homology modeling, MD simulation

# Introduction

Bread wheat (*Triticum aestivum* L.) has been considered one of the initial food crops that have been domesticated as a staple food for thousands of years in the major civilizations of West Asia, North America, and Europe (Giraldo et al., 2019). The area under the cultivation of wheat is 239.63 million hectares in the world and 29.31 million hectares in India, with a total production of 899.37 million metric tonnes in the world and 103.59 million metric tonnes in India (FAO, 2020). The cereal utilization forecast for the years 2020–21 has been raised to 766 million tonnes on a global scale; 54 million tonnes (2%) above the 2019–20 level and 4.3 million tonnes higher than previous reports[1]. The grain yield in wheat is driven by the amount of energy captured by the harvested upper leaves. Hence, it is said that wheat is a limited-source crop. Approximately 75% of the overall yield is contributed by the flag leaf and spike in wheat[2]. As evident from the previous reports, the supply of wheat needs to be increased by 1 billion metric tons to meet the needs of an increasing population. All parts of the plant contribute to the development of spikes in cereal crops (Blade and Baker, 1991). However, it was discovered that the uppermost three leaves determine cereal yield potential due to their importance in grain filling (Bïrsïn, 2005). It was found that the defoliation of flag leaf generated an 18-30% loss in grain yield in wheat (Youssef and Salem, 1976; Banitaba et al., 2007). Therefore it is clear that studying the molecular pathways of flag leaf development is critical for gaining a better understanding of its function and meeting the needs of its exploration to combat the need for food supply.

Photosynthesis is the ultimate process for increasing grain yield in wheat, and the flag leaf is the part of the plant that receives the highest amount of sunlight for the preparation of food. A flag leaf is referred to as the last leaf to emerge from indeterminate plants of the Poaceae family (Palmer et al., 2015). In cereals, the flag leaf is known to provide the largest portion of photassimilates for grain filling



1 (www.agrochart.com)

2 (43bf642e28db4188a97b09ffb580409bd5e7a2a4 @ www.fas.scot)

(Biswal and Kohli, 2013). Wheat is known to be a source limited crop, as its yield is primarily driven through the amount of energy captured by the upper leaves (Koshkin and Tararina, 1989). Morphological characteristics such as the shape and area of the flag leaf contribute to wheat productivity (Liu et al., 2018a). Yield related traits were found to be positively associated with the size of flag leaf in wheat (Fan et al., 2015; Liu et al., 2018a, 2018b). Duwayri (1984) reported that the removal of flag leaves resulted in reduced grain yield and kernel numbers. Different stages occur during the development of a flag leaf, each with its specific function. Flag leaves provide the storage organs with photosynthetic products (Yan et al., 2020), hence it becomes necessary to identify candidate genes associated with different stages of flag leaf development. The synergy of leaf development and environmental factors results in the complex trait of natural senescence (Liu et al., 2016).

Despite the significance of flag leaf in wheat production, a lesser amount of information about their molecular, morphological, and physiological characteristics is available. In the present study, the main objective was to initially identify and then characterize the genes associated with flag leaf development and detailed analysis of proteins encoded in wheat. Through computational analysis, 17 candidate genes were found to be involved in flag leaf development from reference sequences of the wheat genome. These genes were further structurally and functionally annotated through various *in-silico* tools and automated servers. Structural annotation involved the elucidation of gene structure; protein modeling followed by molecular dynamics simulation configuration at different nanoseconds and their physiochemical properties, whereas functional annotation involved gene ontology, phylogenetic relationships, identification of functional domains, molecular interaction networks, and microarray profiling.

# Material and methods:

## 2.1. Structural annotation

### 2.1.1. Identification and chromosomal localization of candidate genes involved in wheat flag leaf development.

The protein sequences of candidate genes associated with the development of flag leaf were retrieved from different model plants such as *Arabidopsis thaliana* and *Oryza sativa* using the NCBI database (www.ncbi.nlm.nih.gov)(Jenuth, 2000). The orthologs of these proteins responsible for flag leaf development in wheat were identified by performing BLASTp (http://plants.ensembl.org/Triticum_aestivum/Tools/Blast) against the EnsemblPlants database (Bolser et al., 2015) with a selection of *T. aestivum* which contains data from different assemblies, namely, PGSBv2.0, Elv1.1, and WeebilV1. The genes associated with these predicted proteins were further annotated for their chromosomal localization in the wheat genome (Kumar et al., 2018b).



### 2.1.2. Identification of gene structure

The Gene Structure Display 2.0 (GSDV2) (http://gsds.gao-lab.org/) server was utilized to explore information regarding the detailed structure of genes. The coding and genomic sequences of the predicted proteins were taken into account for marking 3 major regions of a gene: 3' and 5' UTRs, exons, and introns.

### 2.1.3. Physiochemical properties of candidate proteins

Physiochemical properties are the basic properties of a particular protein, such as the theoretical isoelectric point, instability index, molecular weight and aliphatic index. The ProtParam server (https://web.expasy.org/protparam/) (Garg et al., 2016) was used to analyze all these parameters of candidate proteins associated with flag leaf development in the wheat crop.

### 2.1.4. Homology modeling

3D structural modeling of all 17 candidate proteins associated with the development of flag leaf was performed through the Swiss-Model Server (https://swissmodel.expasy.org/) based on the homology approach. Protein sequences were placed in the target sequence dialog box and a template search was initiated. A template was selected from a set of templates ranging from 3 to 50 concerning PSI BLAST and HHBlits. Based on the similarity, the most suitable template was selected for performing homology-based modeling of candidate genes. The structures of proteins after modeling were further analyzed with UCSF ChimeraX software (https://www.cgl.ucsf.edu/chimerax/) and the ProFunc server (http://www.ebi.ac.uk/thornton-srv/databases/ProFunc/) for proper characterization both at the surface and internal levels. The quality of the protein was checked through the PROCHECK server by dihedral analysis of the Ramachandran plots of predicted candidate proteins.



## 2.2. Annotating candidate genes at the functional level

Functional annotation is the process including annotation of a particular biological function to biomolecules based on a computational approach by comparing the query data with the existing datasets selected in the database. This is one of the most prominent steps after structural annotation of biomolecules (Humann et al., 2019). Functional annotation was performed by analyzing the gene ontology analysis, expression profiling, and molecular simulation studies of the candidate proteins.

### 2.2.1. Gene ontology

Complete functional annotation of the 17 candidate genes was performed at both the nucleotide and protein levels. At the cellular, molecular, and biological levels, gene ontology at the nucleotide level of the candidate genes was performed using the Gene Ontology Resource (http://geneontology.org), Ensembl database

(https://www.ensembleindia.com/), URGI (https://wheat-urgi.versailles.inra.fr/), and Uniparc (https://www.uniprot.org/help/uniparc). For the gene ontology study at the structural level, the modeled protein structures were analyzed with the help of the automated ProFunc server (http://www.ebi.ac.uk/thornton-srv/databases/ProFunc/) for the proper depiction of functions at the cellular, biological, and biochemical levels.

### 2.2.2. Gene expression profiling

The expression profiling of all the candidate genes was performed with the help of Genevestigator (https://genevestigator.com/) at different levels. First, at the anatomical level, depiction was performed on a quantitative basis in different tissues of wheat taking into account the TA_mRNASeq_WHEAT_GL-0 dataset and selecting all 17 candidate genes in heatmap format. Second at 10 different developmental stages, a set of experiments was selected as the desired perturbation for the presence of 17 candidate genes in heatmap format.



### 2.2.3. Experimental validation of candidate genes through expression analysis

#### 2.2.3.1. Plant material and sampling stages

For experimental validation of candidate genes two varieties DBW303 (high yielding) and WH147 (low yielding) were selected. The plants were grown at the research field of wheat and barley section, Department of Genetics and plant breeding, Chaudhary Charan Singh Haryana Agricultural University, Hisar, India. The flag leaf samples of the varieties were collected at 3 different developmental stages flag leaf emergence, fully developed flag leaf and flag leaf senescence (Figure 1).

#### 2.2.3.2. Relative expression of candidate genes in high and low yielding wheat varieties

Total RNA was isolated from 50- 100 mg flag leaf tissue of selected varieties using a Maxwell RSC Plant RNA kit (Promega, USA) according to the manufacturer's

recommendations. A RevertAid cDNA synthesis kit (Thermo Scientific, USA) was used for the synthesis of first-strand cDNA from the total RNA isolated. The primers of all the 17 genes along with actin as an endogenous control were designed with the help of Primer Express program version 3.0 (Applied Biosystem). A detailed list of the primers used is given in the Supplementary Table. 1. Quantitative Real-Time-Polymerase Chain Reaction was performed using a QuantaStudio™ 6 Flex Real-Time PCR Detection System (Applied Biosystem) with PowerUp™ SYBR™ Green PCR Master Mix (Applied Biosystem) with 2 min at 50°C for UDG activation, 10 min at 95°Cfor initial denaturation followed by 40 cycles of (15 sec of denaturation at 95°C, 15 sec of annealing at and extension at 72°C for 1 min). Fold changes were calculated by the $2^{-\Delta\Delta Ct}$ method.

## 2.2.4. Network analysis of candidate genes with native protein and chemical interactors

Protein-protein and protein-chemical interaction network analyses were performed with the help of servers such as GeneMANIA (https://genemania.org/) and the STITCH v 5.0 server (http://stitch.embl.de/), respectively. Network analysis was performed to identify the biomolecules interacting with the candidate genes for proper functional annotation of genes encoding proteins.

## 2.2.4. Molecular dynamics simulation

To evaluate the stability of the predicted 3D structures, MD simulations were performed. Modeled 3D structures from the Swiss-Model server were used as the initial configuration of all simulations. The MD simulations were conducted as per the protocol previously described in (Gajula et al., 2016; Kumar et al., 2016, 2018b, 2018a; Mathpal et al., 2018; Gautam et al., 2019). A minimum 10 Å distance was used between the protein surfaces and the simulation box edges. All the systems were solvated with the TIP3P water model. $Cl^-$ and $Na^+$ were further added to the simulation boxes to neutralize the systems. All unbiased MD simulations were

carried out using GROMACS-2020 (https://www.gromacs.org) with an all-atom CHARMM36 m force field. All the systems were energy minimized and equilibrated with different initial atomic velocities using the following steps: (1)minimization of energy to steepest descent level, (2) restrainment of position (all heavy atoms of protein) NVT (moles (N), volume (V), and temperature (T)) simulation with a restraining force constant of 1000 kJ mol1, and (3) a 500 ps position-restrained NPT (moles (N), pressure (P), and temperature (T)) simulation with a restraining force constant of 1000 kJ mol1.The NPT ensemble was utilized for the simulation production at 20 ns with an average temperature of 300 K via the v-rescale thermostat and Parrinello-Rahman barostat with 2.0 ps as the coupling constant. For the cutoff of Lenard-Jones and other short range electrostatic interactions, a Verletcut-off scheme was employed with a cutoff of 1.0 nm throughout the simulation. The Particle Mesh Ewald (PME) summation method was employed to treat electrostatic interactions over a long-range. The LINCS algorithm was used for the constraint of all hydrogen atoms and the SETTLE algorithm was used for constraining all the bonds and angles of TIP3P water molecules. The root means square deviation (RMSD) of Cα atoms of protein concerning a reference structure was calculated with the GROMACS program "*gmxrms*" by least-square fitting the structure to the reference structure. Principal component analysis (PCA) is a widely used technique to highlight the slowest functional motions of proteins (Bahar et al., 1998). The principal components (PCs) representing the collective motion of the proteins were obtained after diagonalization of the covariance matrix. The eigenvectors and eigenvalues of the covariance matrix represent the principal direction of the motion and the magnitude of motion along with it, respectively. The GROMACS tools "*gmxcovar*" and "*gmxanaeig*" were used for the calculation of the covariance matrix and PC projections.

## 2.3. Phylogenetic analysis

Phylogenetic analysis was conducted to obtain information regarding the relatedness among the 17 candidate proteins, and the phylogenetic tree was constructed with the

help of Mega X (https://www.megasoftware.net/) software using the neighbour-end joining method with 1000 bootstraps.

# Results

## 3.1. Identification and chromosomal localization of candidate genes in the wheat genome associated with flag leaf development

The protein sequences of candidate genes associated with the development of flag leaf were retrieved from different plants such as *Oryza sativa and Arabidopsis thaliana* and orthologs of these proteins responsible for flag leaf development in wheat were identified by BLASTp. All 17 candidate genes that were identified from the EnsemblPlants database were annotated with the help of various bioinformatics tools. The Blastp results yielded more than 50 wheat scaffolds, of which the one with the highest sequence identity with the respective genes was taken as an ortholog for further analysis (Dhaliwal et al., 2014).With each gene queried numerous associated transcripts were found. The full-length transcripts of candidate genes related to flag leaf genes were found to have 67.6% to 99.4% identity with the query sequence. The size of the CDS ranged from 1428 to 4445 bp and the subsequent protein length ranged from 280 to 1124 amino acids (Table 1). In total, 17 flag leaf-associated genes were found to be scattered on chromosomes 1B, 2B, 3D, 4A, 4B, 4D, 5B, 5D, 6B, 7A, 7B and 7D of wheat (Figure 2).

## 3.2. Identification of gene structure

The Gene Structure Display Server (GSDS) v 2.0 was used to elucidate the gene structures of candidate genes associated with the development of the flag leaf. The gene structure comprises exons, introns, and 3' and 5’ untranslated regions. The number of introns ranged from 1 in *TaGATA12-3D* to 22 in *TaNAP1-7B* (Figure 3). The upstream and downstream regions were also analyzed for their detailed localization (Hu et al., 2015). However, the common ancestral origin of different

genes was confirmed, as the exon-intron composition of flag leaf development genes was not different from their homologs.

## 3.3. Physiochemical Properties of Candidate Proteins

The physicochemical properties of candidate proteins associated with the development of the flag leaf were elucidated using the ProtParam server. The molecular weight of translated protein ranged from 31188.61 g/mol (TaSGR-5D) to 151621.01 g/mol (TaNAP1-7B) and the isoelectric point (pI) ranged from 5.37 (TaAct1-4B) to 9.6 (TaNOL-4D). Out of 17 proteins, 5 were found to be stable in nature while 12 were unstable, with their instability index ranging from 40.68 to 67.91 during preliminary analysis. The higher aliphatic index of proteins ranging from 67.10 (TaGATA12-3D) to 97.54 (TaBri1-3D) suggests high stability of proteins over a wider range of temperatures. The gravy score ranged from -0.579 (TaOsh1-4A) to 0.009 (TaPME1-1B) indicating the hydrophilic nature of the proteins (Table 2).



## 3.4. Homology modeling

The modeling was performed based on a homology-based approach through the SWISS-MODEL server (Schwede et al., 2003; Kumar et al., 2018b; Waterhouse et al., 2018). Many templates were found ranging from 3 to 50, concerning PSI-BLAST and HHBlits having a % identity ranging from 17.07 to 90.67. The state of proteins was from monomer to homodimer and homotetramer. Qualitative Model Energy Analysis (QMEAN) values of predicted proteins ranged from -0.28 in TaRCCR1-7D to -5.24 in TaNyc3-7A (Table 3). The derived structures were analyzed further with the help of UCSF ChimeraX1.1 software (Pettersen et al., 2021) for the further depiction of secondary structures such as coils, helices, sheets, and surface features (Figure 4).

The topological architecture of proteins was predicted through the ProFunc server, which elucidates the detailed characteristics of the modeled protein structure and

the ligands attached to it. Ligands such as 4'-deoxy-4'-aminopyridoxal-5'phosphate (PMP), cacodylate (CAC) ions and magnesium (Mg) ions were found to be associated with TaOsl2-2B, TaPME1-1B and TaSRT1-5D, respectively (Figure 5).

## 3.5. Dihedral analysis

Ramachandran dihedral statistics for modeled 3D structures of proteins associated with the development of the flag leaf in wheat with Mol Probity scores ranging from 0.77 (TaAct1-4B) to 2.66 (TaNOL-4D). TaAct1-4B, TaBri1-3D, TaGATA12-3D, TaNfl-2B, TaNyc1-3D, TaPME1-1B, TaPNH1-7B, TaOsh1-4A, TaOsl2-2B, TaRCCR1-7D, TaSCR-5, TaSGR-5D, and TaTSD2-6B were all- approximately zero, indicating good agreement between the modelled structure and an experimental structure of similar size (Table 3). The ProCheck server analysis of the modeled protein revealed a varied percentage of residues under the most favored, generously allowed, additionally allowed, and disallowed regions (Laskowski et al., 1993). The G-score that provides a measure of how normal a structure works with different proteins ranged from -0.32 (TaNyc3-7B) to 0.07 (TaNfl1-2B), indicating that the predicted models were of excellent geometry and were accepted for further analysis (Table 4; Figure S1).



## 3.6. Functional enrichment analysis

Gene ontology enrichment analysis of genes associated with flag leaf development revealed their association with various cellular and metabolic processes. It was found that the candidate genes were involved in several biological and molecular functions, including population maintenance, leaf development, protein phosphorylation, regulation of transcription of various catabolic and anabolic processes that are required for the proper functioning of photosynthesis and nutrient transfer from flag leaf to developing grains, cellular component organization and localization, cell wall modification, and macromolecular metabolism.

## 3.7. Functional elucidation based on protein structure

The Profunc server (Laskowski et al., 2005) was used to explore the functional annotation of genes based on protein structures derived from a homology modeling approach. It revealed the association of these modeled proteins with various cellular, biological, and biochemical processes. Cellular processes included cellular organization and localization of the cytoskeleton, periplasmic spaces, membrane, cytoplasm, intracellular and extracellular regions, Biological processes included metabolic processes such as phosphate and pectin catabolism, as well as carbohydrate and organic acid metabolism. Biochemical processes such as nucleotide, ATP, metal ion, and protein binding, as well as catalytic activities such as hydrolase, oxidoreductase, nuclease, carboxylesterase, aspartyl esterase, and transaminase.

## 3.8. Profiling of gene expression

A microarray TA_mRNASeq_WHEAT_GL-0 dataset of all 17 genes was found to be available on the Genevestigator (Grennan, 2006) platform, which was further utilized for gene expression analysis at different levels.



### 3.8.1. Differential expression in tissues

Expression profiling of all 17 genes revealed their presence in 44 different tissues in wheat, which were analyzed, and it was found that the expression of these genes was higher in the root tip and radicle, shoot apical meristem, seedling, and in the zone undergoing active growth, suggesting that the genes are involved in the development of tissue at the seedling stage as well as at later stages. *TaAct1-4B* was found mostly in the growing parts of the plants, especially in the flag leaf sheath and internodal areas, and it was found to be the most active gene in the flag leaf compared to the rest of the candidate genes. *TaBri1-3D and TaRCCR1-7D* were prominently present in the shoot apex and axillary buds (Figure 6).

### 3.8.2. Expression of candidate genes at different developmental stages

The expression profiles of wheat genes associated with the development of flag leaf were analyzed at ten different developmental stages, including milk development, seedling growth, tillering, anthesis, inflorescence emergence, booting, germination ripening, dough development, , and stem elongation. All the candidate genes either upregulated or downregulated were found to be expressed at all developmental stages. However, the expression of these genes was found to be highly prominent during germination and seed growth, deciphering their role in development; tillering, booting, and anthesis, depicting their role in the development of flag leaf, and functioning as a source–sink pathway at the time of anthesis, when the stored energy in flag leaf starts accumulating in grains (Figure 7).



## 3.8.3. Expression during flag leaf development and senescence

### 3.8.3.1. Flag leaf development

Absolute expression analysis was performed by selecting perturbations where the flag leaf blade was harvested at the beginning of the light period (15 min after lights went on) from Azhurunaya plants grown to Zadoks 37 (flag leaf just visible) in a growth chamber under 16 h light/8 h dark cycles compared to 15 min before lights went on. The higher expression of genes such as *TaNAP1-7B*, *TaNOL-4D, TaNyc1-3D*, *TaOsl2-2B*, *TaSRT1-5D* and *TaTSD2-6B* confirms their involvement in flag leaf development in wheat through processes such as cellular organization, leaf development, and photosynthesis (Figure 8).

### 3.8.3.2. Flag leaf senescence

Selective expression analysis was performed by selecting particular perturbations involving sampling of a 3 cm long section from the middle of the flag leaf blade 26 days after anthesis (dough development) from the main tiller of Bobwhite plants grown under 16 h light at 20°C / 8 h dark at 15°C cycles in 1 L pots filled with Peters

Field Cereal Mix, and 3 days after anthesis, sampling was taken as control (milk development). The chlorophyll content was 10 units higher in the control sample than in the treated sample, which was 26 days after anthesis (Warburton et al., 2002). Similarly, chlorophyll content in the flag leaf was found to increase from the time of heading to the seed setting stage and declined thereafter in cereal crops (Liu et al., 2008; Derkx et al., 2012). The biosynthesis and degradation of chlorophyll are catalyzed by a unique set of enzymes (Reinbothe et al., 2010; Hörtensteiner and Kräutler, 2011). The expression of genes associated with the degradation of chlorophyll is the first molecular indication of the onset of senescence (Hörtensteiner and Kräutler, 2011). As previously stated, the function of these genes was in metabolism, specifically the catabolism of the photosynthetic apparatus and chlorophyll, so the function of these genes can be inferred perfectly from the experiment (Figure 9).

At the molecular level, during the development of the flag leaf, there are different phases controlled by different sets of genes. Phase 1 starts with the increase in the expression of genes involved in the development of the leaf. Phase 2 encounters an increase in the expression of genes associated with the biosynthesis of chlorophyll and other leaf functions. Phase 3 is the most active phase, involving the assimilation of carbon and nitrogen in the leaves, as mature leaves serve as a sink to store nitrogen before the anthesis phase; phase 4 begins with the onset of senescence and is characterized by the decline in leaf chlorophyll content; and upon anthesis, these leaves serve as a source of nitrogen to support the process of grain filling and utilization. Phase 5 involves the remobilization of nutrients from senescing flag leaf to the grain and other developing parts, which will ultimately lead to the complete senescence of the flag leaf. Leaf senescence is known to be an active process until death, with the main functions of recycling and reusing nutrients for the newly developing organs and enhancing the chances of survival of plants under abiotic stress (Figure 10).

## 3.9. The expression profile of candidate genes using RT –PCR

To assess the reliability and validity of *in-silico* expression data and to obtain comprehensive insight into the expression profile of candidate genes in wheat in relation to high yielding and low yielding varieties, - quantitative real-time PCR was performed using gene-specific primers for all 17 candidate genes. The fold change of the genes was analyzed relative to the other two stages of the same variety only.

The expression of *TaAct-4B* was highest in the flag leaf emergence stage of the high yielding wheat variety and similarly in *TaBri-3D, TaNfl1-2B, TaSGR-5D,TaSRT1-5D* and *TaTSD2-6B* indicating their constructive role in the growth of flag leaf. The fold expression of genes such as *TaNyc1-3D, TaNyc3-7A, TaSCR-5B* and *TaOsl2-2B* was more prominent during the senescence of flag leaf revealing their important role in senescence related processes. Not just this expression level of these senescence related genes is much higher in low yielding wheat variety i.e. WH147 compared to the high yield wheat variety DBW303 (Fig 11; 12).

## 3.10. Complex regulatory networks of flag leaf development and associated proteins

### 3.10.1. Network of Protein–Protein Interactions

Due to the unavailability of data for the wheat interactome in GeneMANIA, an interactome study was performed with reference to Arabidopsis. These putative interactor proteins were predicted at the *in-silico* level to have regulatory associated proteins based on physical interactions, shared functional domains, and coexpression. Of 17 proteins, interactome data for 9 proteins were available in *Arabidopsis*. GeneMANIA (Franz et al., 2018) interactome analysis revealed interactions with the 20 most closely related proteins for each gene, allowing the elucidation of different functions based on these interactions.

TaBri1-3D has been discovered to interact with BAK1, CPI1, BSK1, BIK1, CRT3, SERK4, and 14 other proteins. The green lines show their interaction at the genetic level. The interactome analysis of TaBri1-3D revealed that this protein is

involved in steroid metabolism, specifically the brassinosteroid mediated signaling pathway, which is responsible for the negative regulation of cell death in plants. TaGATA12-3D was found to interact with 20 proteins of the same GATA family, including GATA18, GATA4, GATA5, GATA2, etc., which are basically involved in the circadian rhythm of plants. TaNyc1-3D was found to interact with NOL, HCAR, SGR1, SGRL, RCCR and 15 other genes that were found to be involved in chlorophyll metabolic processes and nitrogen-containing compound catabolic processes. TaSRT1-5D was found to interact with SRT2, ETFA, HDA15, NUP62, GLDP1, PHB, DHS, ALS, HACL, PDC, CCA and 9 more genes. These were found to be involved in carboxy-lyase activity, the oxidoreductase complex, mitochondrial respiratory chain complex I, the NADH dehydrogenase complex, and the negative regulation of nitrogen compound metabolic processes. TaOsh1-4A was found to interact with a group of 20 genes, such as GILT, SHM, RHM, ETFB, and ETFQO involved in functions hydrolyase activity, nucleotide biosynthetic processes, and oxidoreductase activity acting on the CH-OH group of donors, NNAD, or NADP as acceptors. TaSGR-5D was found to interact with proteins such as SGRL, NOL, PPH, RCCR, HO1, NYC1, and HCAR, which were found to be involved in chlorophyll metabolic processes, mainly catabolic ones. TaNAP1-7B was found to interact with 20 proteins, including BRK1, FLP, ABIL1, MYB88, PNM1 and HDT2. These proteins were found to be involved in the positive regulation of protein polymerization, cellular component morphogenesis, and cellular component organization. TaSCR-5B was found to be involved in asymmetric cell division by interacting with proteins such as SCL, GASA, PER32, SHR and different SCL elements. TaRCCR1-7D was found to interact with 20 proteins, including ALB, NYC, RVE, SGRL, NOL, PPH, and PAO. These were found to be involved in chlorophyll metabolic processes and cellular nitrogen compound catabolic processes (Figure S2).

These proteins were selected together for interactome analysis and two different clusters were found, one with Nyc1, NOL, SGR, and RCCR, which are involved in chlorophyll metabolic processes, and the second cluster, including NAP, Bri1, and

SCR, which is involved in cellular organization and brassinosteroid mediated cell signaling.

## 3.10.2. Networks of Chemical-Protein Interactions

The chemical-protein interaction analysis was performed with the help of the STITCH v5.0 server against *Hordeum vulgare* (Kuhn et al., 2007). The protein sequence of *TaBri1-3D* was found to interact with manganese and MgATP, *TaGATA12-3D* with MgATP, nitrate, ammonia, nitrite and cycGMP; *TaNOL-4D* with nicotinamine, diphosphate and reduced nitric acid; *TaNyc1-3D* with nicotinamine and reduced nitric acid and TPNH; *TaNyc3-7A* with red chlorophyll, benzoic acid, sphinanine and 7-keto-8-amine; *TaPME1-1B* with methanol, pectate and distilled water; *TaRCCR1-7D* with red chlorophyll, hydrogen, sodium, TPNH, nicotinamine e and p, Se Met; *TaSCR-5B* with R-rolipram and 1,2 dibromo 1; *TaSGR-5D* with CDCs, DMFE and ketoglutrate; *TaSRT1-5D* with magnesium, vitamin B, cabomoyl phosphate, citrulline, ketoglutarate, hydrogen, ammonia, phosphate; *TaTSD2-6B* mifepristone, trichlorobiphosphate, pentachloroniphosphate (Figure S3).

After the analysis of interactions, it was quite evident that most of the proteins were found to be associated with various N containing compounds and enzymes related to nitrogen metabolism. Therefore, the importance of nitrogen and chlorophyll metabolism in flag leaf development was quite evident from the predicted results.

Nitrogen use efficiency depends on nitrogen uptake, assimilation, and remobilization. In cereal crops such as wheat, mature leaves work as a sink to store nitrogen before the stage of anthesis, and upon anthesis, these leaves serve as the source of nitrogen to support the process of grain filling. Plants absorb N in their inorganic forms such as nitrate and ammonia, most of which are assimilated into organic forms. Mature tissue stores all organic and unassimilated inorganic nitrogen, either directly or indirectly utilized by the expanding tissue.

## 3.11. Molecular dynamics simulation of predicted proteins

Molecular dyanamics simulations have been extensively used to explore the conformational behavior of proteins. Here, we performed 20 nanosecond MD simulation studies of seventeen modeled flag leaf genes to understand their structural behavior. To investigate the equilibration and protein stability during the simulations of these proteins, the Cα RMSDs were calculated and monitored over the course of 20 nanosecond simulations. The assessment of the structural change was carried out by the analysis of the RMSDs from the starting structures as a function of simulation time. The resulting RMSD plots, presenting the conformational changes during simulation, showed that all the proteins (except two) achieved equilibrium at ~5 ns and remained stable for a period of 20 ns (Figure 13). These analyses also suggest that there are no large structural changes observed during simulation.



The RMSD values of two proteins, TaNyc1-D and TaSGR-5D, show higher values (>0.6 nm) indicating that these proteins have large conformational changes during the simulation. We used principal component analysis to better understand conformational changes during the simulation. PCA is a widely used method to reveal concerted motions (fluctuations) with large amplitudes (structural variations) from a set of configurations (Hess et al., 2008). All the simulated trajectories were projected along with the first principal component (PC1) which represents the largest structural variations. The motions along PC1 for all the trajectories were rendered (Figure S4). Motions along PC1 showed that the large conformational changes in TaNyc1-D were due to the relative movement of the different subunits, and the intra subunit conformational changes were not significant in TaSGR-5D due to the movement of flexible loops present at the terminal regions.

## 3.12. Phylogenetic analysis

Phylogenetic analysis was performed by using sequences of predicted proteins associated with flag leaf development through Mega-X software (Kumar et al., 2018c). A phylogenetic tree was made using the neighbour-joining method with 1000 bootstraps for inferring evolutionary relationships. Two distinct clusters were obtained, one with the genes involved in developmental processes and the other with the genes involved in degradation processes such as chlorophyll degradation and cell wall degradation. As inferred from Figure 14, the genes involved in the developmental processes made up a larger cluster when compared with the other cluster.

# Discussion:

All 17 candidate genes associated with flag leaf development were characterized with the help of various bioinformatic tools in wheat .Phylogenetic analysis was the most prominent basis for the classification of these genes, under two distinct clusters one with most of the genes associated with development and the other with genes associated with the regulation of senescence in flag leaf.

The first cluster included development-associated genes such as *TaAct1-4B*, *TaNfl1-2B*, *TaPME1-1B*, *TaPNH1-7B*, *TaBri1-3D*, *TaRCCR1-7D*, *TaTSD2-6B*, *TaSRT-5D*and *TaOsh1-4A* except *TaNAP1-7B* and *TaNOL1-4D* whereas the second cluster included senescence-associated genes such as *TaSCR-5B*, *TaNyc3-7A*, *TaSGR-5D*, *TaOsl2-2B*, *TaNyc1-3D,* and *TaGATA12-3D*. Overall, starting from the functional enrichment analysis followed by expression analysis, interaction studies, and structure-based functional analysis; this classification of genes fitted the best in understanding the whole picture of flag leaf development to a larger extent.. The role of these genes as individuals or in collaboration with other genes was too complex to distinctively group them; hence the genes are discussed in accordance with phylogenetic clusters.

TaAct1-4B, a member of the NBD-sugar kinase-Hsp70_act superfamily, plays an important role in cytoskeletal organization, localization, and transport of photoassimilates. Gui et al. (2015) reported that plasmodesmata conductance for the

574 transport of photoassimilates in rice is regulated by the interaction of grain setting
575 defect 1 with *OsACT1* (Gui et al., 2015). Moreover, it was the most prominent gene
576 that was found to be expressed in the flag leaf of wheat, as was deciphered through
577 *in-silico* gene expression analysis and was the most prominent during the flag leaf
578 emergence stage in the high yielding wheat variety. *Nfl* in tobacco was found to
579 specify determinacy for both flowers and leaves in progenitor cells as *Nfl* was found
580 to be expressed in vegetative tissues (Hofer et al., 1997). TaNfl1-2B was found to be a
581 member of the C-LFY-FLO superfamily, expressed predominantly during stages
582 such as inflorescence emergence and germination as studied through gene ontology
583 and expression analysis. The highest amount of TaNfl1-2B was found during the
584 developmental stages of flag leaf in the high yielding wheat variety. Similar results
585 were revealed by Ahearn et al. (2001) signifying the critical role of *Nfl1* in the
586 allocation of meristematic cells that are responsible for the differentiation of lateral
587 structures such as leaves and branches(Ahearn et al., 2001).

588 TaPME1-1B was found to be a pectinesterase and its interaction with pectate
589 was confirmed through STITCH-based chemical protein analysis. Pectin
590 methylesterase (PME) is a carbohydrate esterase family member that cleaves the
591 ester bond between a methyl group and galacturonic acid. The optimal pectin methyl
592 esterification in each cell type is determined by the balance between PME activity
593 and PME inhibitors regulated by posttranslational PME inhibition. Overexpression
594 of PMEI28 was found to result in reduced culm diameter and dwarf phenotypes in
595 transgenic rice plants. It was found to function as a critical structure modulator by
596 regulating the degree of pectin methyl esterification. Impairment in pectin methyl
597 esterification affects physiological properties of the cell wall components and causes
598 abnormal cell extensibility in culm tissue (Nguyen et al., 2017).

599 TaPNH1-7B, an Argonaute (PAZ Piwi domain) protein, found in the cytoplasm
600 and intracellular spaces, has nuclease activity and acts as a positive regulator of leaf
601 development, as evident through its predominant expression in the apex and axillary
602 bud in *in-silico* analysis. The fold expression of TaPNH1-7B was found to be highest
603 during flag leaf emergence followed by fully grown flag leaf stages in the high

yielding wheat variety. The expression of TaPNH1-7B was optimally lower during all stages of flag leaf development in the low yielding wheat variety, so it can be a potent gene to work with to increase the wheat yield. It was found by Nishimura et al. (2002) that *OsPnh not* only functions in S-adenosyl methionine (SAM) maintenance but also leaf formation directly through vascular development. Malformed leaves with abnormal internal vascular structure were observed in antisense *OsPnh1* plants (Nishimura et al., 2002). TaBri1-3D, an LRR from the ribonuclease inhibitor-like superfamily, was found to positively regulate the development of the flag leaf in wheat. Decreased plant height with compact stature, narrow and short leaves, short internodes, decreased brassinosteroid response and expression of BR-related genes were reported in *Brachypodium distachyon* with the BRI1-RNAi mutation(Feng et al., 2015). This supports the increased expression of *TaBri1-3D* during flag leaf development. Although most researchers primarily stress the influence of brassinosteroid signaling genes on factors such as plant height, the impact on leaf architecture is also apparent. Altered leaf architecture, along with other brassinosteroidnsensitive phenotypic traits, was shown in *Uzu 1* a mutant of barley with altered signaling of brassinosteroid due to the exchange of amino acids in the *HvBRI1* gene (Dockter et al., 2014). Similarly, shorter leaf blades and sheaths after the knockdown of *BRI1* homologs were found in maize plants (Kir et al., 2015). In ryegrass genotypes, the deletion in the LpBRI1 locus resulted in significantly narrower leaves compared to genotypes in which the deletion was harbored (Statkevičiūtė et al., 2018). Chemical network analysis of TaBri1-D revealed its involvement in carboxylase and nitrate domains, both for synthase and a transferase. A *dwarf and low tillering* (*dlt*) mutant of rice was characterized, and cloning of the *dlt* gene was performed through map-based cloning. DLT was found to encode a new member of the plant-specific GRAS family. The dwarf phenotype of *dlt* is similar to that of the BR-deficient mutant of rice (Tong et al., 2009).

TaRCCR1-7D was found to be a red chlorophyll catabolite reductase. Through microarray analysis, it was found to be predominantly present during developmental stages such as germination, stem elongation, and booting. The *in-silico* expression

of *TaRCCR1-7D* during the development of the flag leaf was found to be highly increased compared to that of other genes. In contrast, Sakuraba et al. (2013) reported less-pronounced changes in *RCCR* in developing or senescing leaves (Sakuraba et al., 2013). Through PPI and PCI network analysis, TaRCCR1-7D was found to interact with red chlorophyll and genes responsible for its degradation, such as *Nyc, SGRL*, and *NOL*, indicating its potential role in the reduction of chlorophyll catabolic genes and indirectly helping in the development processes.

*TaTSD2-6B* expression, which is a member of the methyltransferase 29 family, was found to be increased during the emergence of the flag leaf and unaffected during the senescence stage when analyzed through GENEVESTIGATOR. Similar results were found through expression analysis in high yielding wheat varieties. Through chemical network analysis, *TaTSD2-6B* was found to be interact with reduced cell adhesion and noncordial shoot development, similar to what was observed in the mutant of the *TSD2* gene (Krupková et al., 2007).

TaSRT-5D, an inter-alpha trypsin inhibitor, was involved in stem elongation and an increase in its expression during flag leaf emergence was also elucidated through microarray analysis. TaSRT1-5D was found to be most prominent in the high yielding wheat variety during flag leaf emergence. Through network analysis, it was found to interact with intermediates of different metabolic cycles, such as the citric acid cycle. *OsSRT1*, one of the homolog of Silent information regulator 2 (*SIR2*) in rice, was found to negatively regulate the process of leaf senescence by repressing the expression of the biosynthetic genes of the leaf senescence metabolic cascade and partially through H3K9 deacetylation of *OsPME1* (Fang et al., 2016). *TaOsh1-4A*, a homeobox family member, is highly important for the development of the plant. An Osh15 mutant revealed the importance of the KNOX gene in the self-regulation of other genes as well as SAM (Tsuda et al., 2011).

Of all the genes in cluster 1 discussed before, *TaNAP1-7B* and *TaNOL1-4D* were the only exceptions that were found to be not associated with developmental processes. *TaNAP1-7B*, expression increased during the emergence stage of flag leaf development. It was found to be involved in cellular component morphogenesis and

organization. *OsNAP* was found to act as an important link between ABA and leaf senescence in rice. The mutant named *ps1,* i.e., a gain of function mutant, significantly exhibited premature senescence, in which the expression of ABA biosynthesis genes was found to be affected. The knockdown of *OsNAP* was found to produce an obvious delay in the process of senescence, which most importantly slowed the decrease in the functional photosynthetic capacity and highly influenced the seed setting ratio to a higher extent (Liang et al., 2014). The expression analysis of TaNAP1-7B deciphered its negative role in stay-green character in wheat, as it was found to be highest during the flag leaf senescence stage of the low yielding variety and lowest during that in the high yielding variety. TaNOL1-4D was found to be a member of the SDR family, whose expression most likely increased during flag leaf senescence (Kusaba et al., 2007; Park et al., 2007). Through network analysis, it was found to play an important role in carboxylic acid synthesis. When analyzed using microarray, its increased level of expression during senescence was quite evident through its increased level of expression during senescence. TaNOL-4D was also found to be highly expressed in the low yield wheat variety during flag leaf senescence; hence its role in senescence is quite clear. The *Nyc3* mutant was found to retain more chlorophyll a and b content than the wild-type and a significant decrease in senescence parameters during dark incubation suggested that it is a nonfunctional stay-green mutant. In addition, a small amount of chlorophyll a, pheophytin a, and Mg derivative without $^{2+}$ in its tetrapyrrole ring, accumulated in the senescent leaves of the *nyc3* mutant (Sato et al., 2009). Similarly, its expression was highest during the flag leaf senescence stage in the low yield wheat variety.

Regardless of decrease in leaf functionality, the retention of chlorophyll during leaf senescence was increased in the mutant of the stay-green *SGR* gene in rice and its orthologs in A. thaliana (Nonyellowing), *Festuca pratensis* (*SENESCENCE-INDUCED-DEFICIENCY*), tomato (*GREEN-FRESH*), pepper (*CHLOROPHYLL RETAINER*) and pea (*I*; known as Mendel's green cotyledon gene) (Armstead et al., 2006; Jiang et al., 2007; Kusaba et al., 2007; Park et al., 2007; Aubry et al., 2008; Barry et al., 2008). *SGR* overexpression in rice

seedlings resulted in the generation of singlet oxygen and activation of other reactive oxygen species and resulted in a chlorophyll-dependent regional cell death phenotype in the leaves (Jiang et al., 2011). It was evident that *OsSGR*, a member of the stay-green superfamily, plays an important role in the regulation of chlorophyll degradation, and the changes in the transcript expression levels of *OsSGR* are reflected in the regulation of jasmonic acid and cytokinin on chlorophyll degradation and leaf senescence. It was found to catalyze a key conversion from a red chlorophyll catabolite to a primary fluorescent catabolite during the degradation of chlorophyll (Liu et al., 2016). Chlorophyll was found to be degraded through the induction of light-harvesting chlorophyll a/b protein complex II (LHCPII) disassembly leading to the degradation of chlorophyll and chlorophyll-free LHCPII by proteases and catabolic enzymes, respectively (Park et al., 2007). However, the expression was highest in the flag leaf emergence stage at the high yield and flag leaf senescence stages in the low yield wheat variety depicting its contrary nature. TaOsl2-2B, an aspartate aminotransferase, was deciphered from network analysis and gene ontology analysis as being connected to various nitrogen-containing compounds. The overexpressed *OsL2* fusion protein in recombinant E. coli showed pyruvate-dependent-aminobutyric acid (GABA) transaminase activity. Induced *Osl2*-specific transcripts were found to be induced in the leaves that were senescing and the chronological profile of accumulation of Osl2 protein was found to be linked with that of pyruvate-dependent GABA transaminase activity in the rice leaf (Ansari et al., 2005). The expression of *TaOsl2-2B* was also found to be elevated during the senescence of flag leaf specifically in the low yield wheat variety as well as through microarray analysis indicating its significance as a senescence-associated gene.

*TaNyc1-3D* was found to interact with senescence-associated genes such as HCAR, SGR and various nitrogen metabolites. Its expression was also prominently increased during flag leaf senescence. *Nyc1* encodes a membrane-localized short-chain dehydrogenase/reductase (SDR) that represents a chlorophyll b reductase that is required to catalyze the initial step of chlorophyll degradation. The *Nyc1* mutant, when analyzed, showed stay-green characters phenotypically. Similar stay-green

phenotypes were reported in rice *nol* mutant such as *nyc1* mutants i.e., confirming that chlorophyll b degradation was selectively retained during senescence, resulting in the retention of thylakoid grana even at a later stage of senescence. It was found to severely inhibit the light-harvesting complex(Sato et al., 2009).

When *overexpressed* in a semi-dwarf rice variety, *OsGATA12,* a zinc-finger transcription factor, caused an increase in the greenness of the leaf, a reduction in the tiller number and other yield related attributes. The transgenic plants were found to be comparatively distinct from the wild type due to a significant increase in yield per area and harvest index as a result of reduced tillering. The increased greenness observed in the transformed plants was mostly due to decreased chlorophyll degradation along with chlorophyll synthesis, as the expression of genes involved in the degradation pathway of chlorophyll was also reduced (Lu et al., 2017). So *TaGATA12-3D* was found to regulate the processes of catabolism in plants, as revealed through gene ontology analysis.

Functional enrichment analysis revealed the enzymatic functions of *TaPME1-1B, TaNyc3-7A, TaNyc-3D1, TaNOL-4D, TaTSD2-6B, TaOsl2-2B* and *TaRCCR1-7D* and the regulatory functions of *TaPnNH1-7B*, *TaBri1-3D*, *TaOsh1-4A*, *TaSRT1-5D* and *TaAct1-4B* in aiding cytoskeleton organization. Overexpression of beneficial genes for photosynthetic activity, nutrient transport, and remaining green in nature, or creation of mutant lines with defective expression of genes involved in chlorophyll degradation and PCD, which are indirectly responsible for senescence. Both approaches can be given as individual trials or can be combined to obtain the best results regarding higher yields. It is quite evident from the results of MD simulations that all the candidate genes except *TaNyc1-3D* and *TaSGR-5D* were found to be stable under 20s RMAD analysis and hence can be validated and used for further applications.

# Conclusion and outlook for the future

With the concomitant development of genetic and molecular studies for the development of plants, a huge amount of understanding about the expression

patterns of genes, their cellular locations and molecular functions. It is obvious to realize that *in-silico* approaches, involving the use of bioinformatics tools remain a cost-effective method to make rapid analysis regarding the expected effect of genes; the more factors that are taken into account, the more accurate the prediction will be. Therefore, in this article, we performed the complete structural and functional annotation of genes related to different developmental stages of flag leaf, so that direct or indirect higher grain yield can be achieved in the future by exploiting the information of these genes. Several genes associated with the development of flag leaf were identified and mapped to the genome. From the variations in characteristics from the structure of genes to microarray gene expression studies and phylogeny, it is quite evident that there is a great deal of complexity within the processes controlled by these genes. The 3D structures of proteins encoded by candidate genes were formed through a homology modeling-based approach. Modeled 3D structures of all the proteins were evaluated by using dihedral analysis of the Ramachandran plot. To assess the stability of modeled structures molecular dynamics simulations after energy minimization were performed. By analyzing the results of both MD and homology modeling the results were found to be consistent with the known set of investigational data. Based on our results; it has been concluded that these genes can be considered important candidates for the regulation of the development of the flag leaf in wheat. Through the thorough investigation of these genes associated with different processes such as leaf emergence, development, nutrient remobilization and senescence. The results indicated that the improvement in yield production can be attained by regulating the genes associated with the source–sink pathway and senescence of flag leaf. Leaf senescence is a major determinant of yield in many cereal crops. Stay-green, delayed senescence is associated with the retention of high yield increments due to higher photosynthetic capacity during the active stage (Gentinetta et al., 1986; Thomas and Howarth, 2000). The stay-green sorghum variety B35 has been reported by Rosenow (1983). It was found to show postflowering and drought resistance with a high contribution to stable and high yield production (Rosenow, 1983). Through gene

expression analysis it was clear that by enhancing the expression of genes such as TaSRT1-5D, TaPNH1-7B, and TaNfl1-2B and by downregulating genes such as TaNAP1-7B, TaNOL-4Dand TaOsl-2B higher-yielding wheat varieties could be generated. Therefore the data regarding the candidate genes can be utilized to manipulate these complex processes such as the source–sink pathway and senescence for the enhancement of yield in wheat. Despite comprehensive analysis in the current study, there is still much room for improvement before a complete array of regulation of these complex processes involved in flag leaf development through validating these genes through reverse genetics and biotechnological approaches.

## Data Availability Statement

The data supporting this study will be provided by the authors.

## Author Contributions

SM performed bioinformatics data analysis.NA performed the molecular dynamics simulation of modeled structures.SM, PK, YS, PS, NL and VS drafted the manuscript. The UK served as the principal investigator and also revised the manuscript. OP, AK, RM, KP, PB, VP, and ID reviewed the manuscript. All authors agreed to the final manuscript.

## Conflict of Interest

The authors stated that the study was conducted in the absence of a commercial or financial relationship that could be considered a potential competing interest.

## Acknowledgments

The corresponding author is highly grateful to the Head, Department of Molecular Biology, Biotechnology & Bioinformatics, and Directorate of Research, CCS Haryana Agricultural University for providing all the necessary facilities during the course of this work. This work was supported by SPARC, Ministry of Education, GOI in

collaboration with University of Massachusetts, Amherst (SPARC/2018-2019/P854/SL).

# References

43bf642e28db4188a97b09ffb580409bd5e7a2a4 @ www.fas.scot Available at: https://www.fas.scot/news/the-importance-of-protecting-the-flag-leaf-in-winter-wheat/.

7751a47505ef5f64d6f8117bd892e386d0af972e @ www.ncbi.nlm.nih.gov Available at: https://www.ncbi.nlm.nih.gov.

Ahearn, K. P., Johnson, H. A., Weigel, D., and Wagner, D. R. (2001). NFL1, a Nicotiana tabacum LEAFY-like gene, controls meristem initiation and floral structure. *Plant Cell Physiol.* 42, 1130–1139.

Ansari, M. I., Lee, R.-H., and Chen, S.-C. G. (2005). A novel senescence-associated gene encoding $γ$-aminobutyric acid (GABA): pyruvate transaminase is upregulated during rice leaf senescence. *Physiol. Plant.* 123, 1–8.

Armstead, I., Donnison, I., Aubry, S., Harper, J., Hörtensteiner, S., James, C., et al. (2006). From crop to model to crop: identifying the genetic basis of the staygreen mutation in the Lolium/Festuca forage and amenity grasses. *New Phytol.* 172, 592–597.

Aubry, S., Mani, J., and Hörtensteiner, S. (2008). Stay-green protein, defective in Mendel's green cotyledon mutant, acts independent and upstream of pheophorbide a oxygenase in the chlorophyll catabolic pathway. *Plant Mol. Biol.* 67, 243–256.

Bahar, I., Atilgan, A. R., Demirel, M. C., and Erman, B. (1998). Vibrational dynamics of folded proteins: significance of slow and fast motions in relation to function and stability. *Phys. Rev. Lett.* 80, 2733.

Banitaba, A., Naderi, M., Javanmard, H., and Emami, B. (2007). Effect of flag leaf and awn removal on vegetative traits, grain yield and yield components of bread wheat (Triticum aestivum L.).

Barry, C. S., McQuinn, R. P., Chung, M.-Y., Besuden, A., and Giovannoni, J. J. (2008). Amino acid substitutions in homologs of the STAY-GREEN protein are responsible for the green-flesh and chlorophyll retainer mutations of tomato and pepper. *Plant Physiol.* 147, 179–187.

Birsin, M. A. (2005). Effects of removal of some photosynthetic structures on some yield components in wheat. *J. Agric. Sci.* 11, 364–367.

Biswal, A. K., and Kohli, A. (2013). Cereal flag leaf adaptations for grain yield under drought: knowledge status and gaps. *Mol. Breed.* 31, 749–766.

Blade, S. F., and Baker, R. J. (1991). Kernel Weight Response to Source-Sink Changes in Spring Wheat. *Crop Sci.* 31, 1117–1120.

Bolser, D. M., Kerhornou, A., Walts, B., and Kersey, P. (2015). Triticeae resources in ensembl plants. *Plant Cell Physiol.* 56, e3--e3.

Derkx, A. P., Orford, S., Griffiths, S., Foulkes, M. J., and Hawkesford, M. J. (2012). Identification of differentially Senescing mutants of wheat and impacts on yield, biomass and nitrogen Partitioning F. *J. Integr. Plant Biol.* 54, 555–566.

Dhaliwal, A. K., Mohan, A., and Gill, K. S. (2014). Comparative analysis of ABCB1 reveals novel structural and functional conservation between monocots and dicots. *Front. Plant Sci.* 5, 657.

Dockter, C., Gruszka, D., Braumann, I., Druka, A., Druka, I., Franckowiak, J., et al. (2014). Induced variations in brassinosteroid genes define barley height and sturdiness, and expand the green revolution genetic toolkit. *Plant Physiol.* 166, 1912–1927.

Duwayri, M. (1984). Effect of flag leaf and awn removal on grain yield and yield components of wheat grown under dryland conditions. *F. Crop. Res.* 8, 307–313.

Fan, X., Cui, F., Zhao, C., Zhang, W., Yang, L., Zhao, X., et al. (2015). QTLs for flag leaf size and their influence on yield-related traits in wheat (Triticum aestivum L.). *Mol. Breed.* 35, 1–16.

Fang, C., Zhang, H., Wan, J., Wu, Y., Li, K., Jin, C., et al. (2016). Control of leaf senescence by an MeOH-jasmonates cascade that is epigenetically regulated by OsSRT1 in rice. *Mol. Plant* 9, 1366–1378.

fao-the-estimate-for-global-cereal-production-in-2020-raised-sharply-while-early-prospects-for-cereal-production-in-2021-are-positive @ www.agrochart.com Available at: https://www.agrochart.com/en/news/7340/fao-the-estimate-for-global-cereal-production-in-2020-raised-sharply-while-early-prospects-for-cereal-production-in-2021-are-positive.html.

FAO (2020). En @ Www.Fao.Org. Available at: http://www.fao.org/fishery/statistics/software/fishstatj/en.

Feng, Y., Yin, Y., and Fei, S. (2015). Down-regulation of BdBRI1, a putative brassinosteroid receptor gene produces a dwarf phenotype with enhanced drought tolerance in Brachypodium distachyon. *Plant Sci.* 234, 163–173.

Franz, M., Rodriguez, H., Lopes, C., Zuberi, K., Montojo, J., Bader, G. D., et al. (2018). GeneMANIA update 2018. *Nucleic Acids Res.* 46, W60--W64.

Gajula, M. N. V. P., Kumar, A., and Ijaq, J. (2016). Protocol for molecular dynamics simulations of proteins. *Bio-protocol* 6, e2051--e2051.

Garg, V. K., Avashthi, H., Tiwari, A., Jain, P. A., Ramkete, P. W., Kayastha, A. M., et al. (2016). MFPPI--multi FASTA ProtParam interface. *Bioinformation* 12, 74.

Gautam, T., Saripalli, G., Gahlaut, V., Kumar, A., Sharma, P. K., Balyan, H. S., et al. (2019). Further studies on sugar transporter (SWEET) genes in wheat (Triticum aestivum L.). *Mol. Biol. Rep.* 46, 2327–2353. doi:10.1007/s11033-019-04691-0.

Gentinetta, E., Ceppl, D., Lepori, C., Perico, G., Motto, M., and Salamini, F. (1986). A major gene for delayed senescence in maize. Pattern of photosynthates accumulation and inheritance. *Plant Breed.* 97, 193–203.

Giraldo, P., Benavente, E., Manzano-Agugliaro, F., and Gimenez, E. (2019). Worldwide research trends on wheat and barley: A bibliometric comparative analysis. *Agronomy* 9, 352.

Grennan, A. K. (2006). Genevestigator. Facilitating web-based gene-expression analysis. *Plant Physiol.* 141, 1164–1166.

Gui, J., Zheng, S., Shen, J., and Li, L. (2015). Grain setting defect1 (GSD1) function in rice depends on S-acylation and interacts with actin 1 (OsACT1) at its C-terminal. *Front. Plant Sci.* 6, 804.

Hofer, J., Turner, L., Hellens, R., Ambrose, M., Matthews, P., Michael, A., et al. (1997). UNIFOLIATA regulates

leaf and flower morphogenesis in pea. *Curr. Biol.* 7, 581–587.

Hörtensteiner, S., and Kräutler, B. (2011). Chlorophyll breakdown in higher plants. *Biochim. Biophys. Acta (BBA)-Bioenergetics* 1807, 977–988.

Hu, B., Jin, J., Guo, A.-Y., Zhang, H., Luo, J., and Gao, G. (2015). GSDS 2.0: an upgraded gene feature visualization server. *Bioinformatics* 31, 1296–1297.

Humann, J. L., Lee, T., Ficklin, S., and Main, D. (2019). "Structural and functional annotation of eukaryotic genomes with GenSAS," in *Gene prediction* (Springer), 29–51.

Jenuth, J. P. (2000). "The ncbi," in *Bioinformatics methods and protocols* (Springer), 301–312.

Jiang, H., Chen, Y., Li, M., Xu, X., and Wu, G. (2011). Overexpression of SGR results in oxidative stress and lesion-mimic cell death in rice seedlings. *J. Integr. Plant Biol.* 53, 375–387.

Jiang, H., Li, M., Liang, N., Yan, H., Wei, Y., Xu, X., et al. (2007). Molecular cloning and function analysis of the stay green gene in rice. *Plant J.* 52, 197–209.

Kir, G., Ye, H., Nelissen, H., Neelakandan, A. K., Kusnandar, A. S., Luo, A., et al. (2015). RNA interference knockdown of BRASSINOSTEROID INSENSITIVE1 in maize reveals novel functions for brassinosteroid signaling in controlling plant architecture. *Plant Physiol.* 169, 826–839.

Koshkin, E. I., and Tararina, V. V (1989). Yield and source/sink relations of spring wheat cultivars. *F. Crop. Res.* 22, 297–306.

Krupková, E., Immerzeel, P., Pauly, M., and Schmülling, T. (2007). The TUMOROUS SHOOT DEVELOPMENT2 gene of Arabidopsis encoding a putative methyltransferase is required for cell adhesion and co-ordinated plant development. *Plant J.* 50, 735–750.

Kuhn, M., von Mering, C., Campillos, M., Jensen, L. J., and Bork, P. (2007). STITCH: interaction networks of chemicals and proteins. *Nucleic Acids Res.* 36, D684--D688.

Kumar, A., Kumar, S., Kumar, A., Sharma, N., Sharma, M., Singh, K. P., et al. (2018a). Homology Modeling, Molecular Docking and Molecular Dynamics Based Functional Insights into Rice Urease Bound to Urea. *Proc. Natl. Acad. Sci. India Sect. B - Biol. Sci.* 88, 1539–1548. doi:10.1007/s40011-017-0898-0.

Kumar, A., Kumar, S., Kumar, U., Suravajhala, P., and Gajula, M. N. V. P. (2016). Functional and structural insights into novel DREB1A transcription factors in common wheat (Triticum aestivum L.): A molecular modeling approach. *Comput. Biol. Chem.* 64, 217–226.

Kumar, A., Sharma, M., Kumar, S., Tyagi, P., Wani, S. H., Gajula, M. N. V. P., et al. (2018b). Functional and structural insights into candidate genes associated with nitrogen and phosphorus nutrition in wheat (Triticum aestivum L.). *Int. J. Biol. Macromol.* 118, 76–91.

Kumar, S., Stecher, G., Li, M., Knyaz, C., and Tamura, K. (2018c). MEGA X: molecular evolutionary genetics analysis across computing platforms. *Mol. Biol. Evol.* 35, 1547.

Kusaba, M., Ito, H., Morita, R., Iida, S., Sato, Y., Fujimoto, M., et al. (2007). Rice NON-YELLOW COLORING1 is involved in light-harvesting complex II and grana degradation during leaf senescence. *Plant Cell* 19, 1362–1375.

Laskowski, R. A., MacArthur, M. W., Moss, D. S., and Thornton, J. M. (1993). PROCHECK: a program to check

the stereochemical quality of protein structures. *J. Appl. Crystallogr.* 26, 283–291.

Laskowski, R. A., Watson, J. D., and Thornton, J. M. (2005). ProFunc: a server for predicting protein function from 3D structure. *Nucleic Acids Res.* 33, W89--W93.

Liang, C., Wang, Y., Zhu, Y., Tang, J., Hu, B., Liu, L., et al. (2014). OsNAP connects abscisic acid and leaf senescence by fine-tuning abscisic acid biosynthesis and directly targeting senescence-associated genes in rice. *Proc. Natl. Acad. Sci.* 111, 10013–10018.

Liu, K., Xu, H., Liu, G., Guan, P., Zhou, X., Peng, H., et al. (2018a). QTL mapping of flag leaf-related traits in wheat (Triticum aestivum L.). *Theor. Appl. Genet.* 131, 839–849. doi:10.1007/s00122-017-3040-z.

Liu, L., Xu, W., Hu, X., Liu, H., and Lin, Y. (2016). W-box and G-box elements play important roles in early senescence of rice flag leaf. *Sci. Rep.* 6, 1–9. doi:10.1038/srep20881.

Liu, L., Zhou, Y., Zhou, G., Ye, R., Zhao, L., Li, X., et al. (2008). Identification of early senescence-associated genes in rice flag leaves. *Plant Mol. Biol.* 67, 37–55. doi:10.1007/s11103-008-9300-1.

Liu, Y., Tao, Y., Wang, Z., Guo, Q., Wu, F., Yang, X., et al. (2018b). Identification of QTL for flag leaf length in common wheat and their pleiotropic effects. *Mol. Breed.* 38, 1–11.

Lu, G., Casaretto, J. A., Ying, S., Mahmood, K., Liu, F., Bi, Y.-M., et al. (2017). Overexpression of OsGATA12 regulates chlorophyll content, delays plant senescence and improves rice yield under high density planting. *Plant Mol. Biol.* 94, 215–227.

Mathpal, P., Kumar, U., Kumar, A., Kumar, S., Malik, S., Kumar, N., et al. (2018). Identification, expression analysis, and molecular modeling of Iron-deficiency-specific clone 3 (Ids3)-like gene in hexaploid wheat. *3 Biotech* 8, 1–11.

Nguyen, H. P., Jeong, H. Y., Jeon, S. H., Kim, D., and Lee, C. (2017). Rice pectin methylesterase inhibitor28 (OsPMEI28) encodes a functional PMEI and its overexpression results in a dwarf phenotype through increased pectin methylesterification levels. *J. Plant Physiol.* 208, 17–25.

Nishimura, A., Ito, M., Kamiya, N., Sato, Y., and Matsuoka, M. (2002). OsPNH1 regulates leaf development and maintenance of the shoot apical meristem in rice. *Plant J.* 30, 189–201.

Palmer, N. A., Donze-Reiner, T., Horvath, D., Heng-Moss, T., Waters, B., Tobias, C., et al. (2015). Switchgrass (Panicum virgatum L) flag leaf transcriptomes reveal molecular signatures of leaf development, senescence, and mineral dynamics. *Funct. Integr. Genomics* 15, 1–16. doi:10.1007/s10142-014-0393-0.

Park, S.-Y., Yu, J.-W., Park, J.-S., Li, J., Yoo, S.-C., Lee, N.-Y., et al. (2007). The senescence-induced staygreen protein regulates chlorophyll degradation. *Plant Cell* 19, 1649–1664.

Pettersen, E. F., Goddard, T. D., Huang, C. C., Meng, E. C., Couch, G. S., Croll, T. I., et al. (2021). UCSF ChimeraX: Structure visualization for researchers, educators, and developers. *Protein Sci.* 30, 70–82.

Reinbothe, C., El Bakkouri, M., Buhr, F., Muraki, N., Nomata, J., Kurisu, G., et al. (2010). Chlorophyll biosynthesis: spotlight on protochlorophyllide reduction. *Trends Plant Sci.* 15, 614–624.

Rosenow, D. T. (1983). Breeding for resistance to root and stalk rots in Texas. *Sorghum root Stalk rots, a Crit. Rev. Patancheru, AP, India ICRISTAT*, 209–217.

Sakuraba, Y., Kim, Y.-S., Yoo, S.-C., Hörtensteiner, S., and Paek, N.-C. (2013). 7-Hydroxymethyl chlorophyll a

reductase functions in metabolic channeling of chlorophyll breakdown intermediates during leaf senescence. *Biochem. Biophys. Res. Commun.* 430, 32–37.

Sato, Y., Morita, R., Katsuma, S., Nishimura, M., Tanaka, A., and Kusaba, M. (2009). Two short-chain dehydrogenase/reductases, NON-YELLOW COLORING 1 and NYC1-LIKE, are required for chlorophyll b and light-harvesting complex II degradation during senescence in rice. *Plant J.* 57, 120–131.

Schwede, T., Kopp, J., Guex, N., and Peitsch, M. C. (2003). SWISS-MODEL: an automated protein homology-modeling server. *Nucleic Acids Res.* 31, 3381–3385.

Statkevičiūtė, G., Kemešytė, V., Aleliūnas, A., Jonavičienė, K., and Brazauskas, G. (2018). Daugiametės svidrės LpBRI1 geno sekos polimorfizmo ir lapų architektūros sąsajų analizė. *Zemdirbyste* 105, 33–38. doi:10.13080/z-a.2018.105.005.

Thomas, H., and Howarth, C. J. (2000). Five ways to stay green. *J. Exp. Bot.* 51, 329–337.

Tong, H., Jin, Y., Liu, W., Li, F., Fang, J., Yin, Y., et al. (2009). DWARF AND LOW-TILLERING, a new member of the GRAS family, plays positive roles in brassinosteroid signaling in rice. *Plant J.* 58, 803–816.

Tsuda, K., Ito, Y., Sato, Y., and Kurata, N. (2011). Positive autoregulation of a KNOX gene is essential for shoot apical meristem maintenance in rice. *Plant Cell* 23, 4368–4381.

Warburton, M., Skovmand, B., and Mujeeb-Kazi, A. (2002). The molecular genetic characterization of the'Bobwhite'bread wheat family using AFLPs and the effect of the T1BL. 1RS translocation. *Theor. Appl. Genet.* 104, 868–873.

Waterhouse, A., Bertoni, M., Bienert, S., Studer, G., Tauriello, G., Gumienny, R., et al. (2018). SWISS-MODEL: homology modelling of protein structures and complexes. *Nucleic Acids Res.* 46, W296--W303.

Yan, X., Zhao, L., Ren, Y., Zhang, N., Dong, Z., and Chen, F. (2020). Identification of genetic loci and a candidate gene related to flag leaf traits in common wheat by genome-wide association study and linkage mapping. *Mol. Breed.* 40, 1–15.

Youssef, S., and Salem, A. (1976). Contribution of individual plant parts to grain yield and protein content and quality of two wheat varieties [Giza 155, Chenab] differing in protein content. *Al-Bohouth Azziraiya*.



# Figures and Tables

**Graphical abstract**

**Figure 1.** Morphology of flag leaf of DBW303 and WH147 at different stages of sample collection

**Figure 2.** Distribution of 17 candidate genes associated with the development of the flag leaf on different chromosomes of wheat

**Figure 3.** Distribution of exons and introns, along with upstream and downstream regions in wheat candidate genes associated with flag leaf development (predicted by the GSDV v2.0 server)

**Figure 4.** Homology-based models (molecular graphical images) produced using UCSF Chimera

**Figure 5.** Localization of ligands interacting with the modeled protein structure through ChimeraX

**Figure 6.** Hierarchical clustering of wheat genes based on their expression in 44 different tissues

**Figure 7.** Hierarchical clustering of wheat genes based on their expression in 10 different development stages.

**Figure 8.** Hierarchical clustering of wheat genes based on their expression under the emergence stage in flag leaf

**Figure 9.** Hierarchical clustering of wheat genes based on their expression under senescence perturbations

**Figure 10.** Developmental stages of flag leaf in wheat

**Figure 11.** Expression of 9 candidate genes in 3 different stages (A: Flag leaf emergence, B: Fully developed flag leaf and C: Flag leaf at the time of senescence) in high yielding (DBW303) and low yielding (WH147) wheat varieties.

**Figure 12.** Expression of 8 candidate genes in 3 different stages (A: Flag leaf emergence, B: Fully developed flag leaf and C: Flag leaf at the time of senescence) in high yielding (DBW303) and low yielding (WH147) wheat varieties.

**Figure 13.** MD simulations of genes associated with flag leaf development

**Figure 14.** Phylogenetic tree of proteins associated with the development of flag leaf developed through MegaX software

**Table 1.** List of identified flag leaf development associated genes along with their basic characteristics elucidated with help EnsemblPlants database

| S No. | Gene | Ensembl ID | Location | Cellular Location | CDS | AA |
|---|---|---|---|---|---|---|

| | | | | | | |
|---|---|---|---|---|---|---|
| **1** | ***TaAct1-4B*** | TraesCS4B02G050600 | 4B | Cytoskeleton | 1982 | 385 |
| **2** | ***TaBri1-3D*** | TraesCS3D02G246500 | 3D | Endosome, membrane | 4445 | 1124 |
| **3** | ***TaGATA12-3D*** | TraesCS3D02G274600 | 3D | Nucleus | 1747 | 386 |
| **4** | ***TaNAP1-7B*** | TraesCS7B02G167200 | 7B | Cytoplasm | 4074 | 1357 |
| **5** | ***TaNfl1-2B*** | TraesCS2B02G464200 | 2B | Nucleus | 1428 | 392 |
| **6** | ***TaNOL-4D*** | TraesCS4D02G012100 | 4D | Chloroplast thylakoid | 1432 | 345 |
| **7** | ***TaNyc1-3D*** | TraesCS3D02G159800 | 3D | Plastid, integral part of membrane | 2121 | 499 |
| **8** | ***TaNyc3-7A*** | TraesCS7A02G338900 | 7A | Chloroplast | 2258 | 547 |
| **9** | ***TaOsh1-4A*** | TraesCS4A02G256700 | 4A | Nucleus | 1616 | 362 |
| **10** | ***TaOsl2-2B*** | TraesCS2B02G440400 | 2B | Mitochondria | 1536 | 511 |
| **11** | ***TaPME1-1B*** | TraesCS1B02G274500 | 1B | Cytoplasm | 1981 | 555 |
| **12** | ***TaPNH1-7B*** | TraesCS7B02G256500 | 7B | Cytoplasm | 3410 | 956 |
| **13** | ***TaRCCR1-7D*** | TraesCS7D02G492300 | 7D | Chloroplast | 1565 | 455 |
| **14** | ***TaSCR-5B*** | TraesCS5B02G143100 | 5B | Nucleus | 2339 | 638 |
| **15** | ***TaSGR-5D*** | TraesCS5D02G325900 | 5D | Chloroplast, Mitochondria | 1798 | 280 |
| **16** | ***TaSRT1-5D*** | TraesCS5D02G066000 | 5D | Nucleus | 2870 | 755 |
| **17** | ***TaTSD2-6B*** | TraesCS6B02G348700 | 6B | Golgi apparatus | 2961 | 660 |

**Table 2.** Physiochemical properties of candidate proteins associated with the development of flag leaf through ProtParam server.

| S No. | Protein | Molecular Weight | Theoretical Isoelectric point | Instability Index | Aliphatic Index | Gravy | Stability |
|---|---|---|---|---|---|---|---|
| **1** | **TaAct1-4B** | 42740.95 | 5.37 | 35.52 | 85.87 | -0.151 | Stable |
| **2** | **TaBri1-3D** | 120078.06 | 5.8 | 33.29 | 97.54 | -0.014 | Stable |
| **3** | **TaGATA12-3D** | 40961.89 | 5.96 | 67.28 | 67.1 | -0.445 | Unstable |
| **4** | **TaNAP1-7B** | 151621.01 | 6.35 | 48.48 | 94.48 | -0.147 | Unstable |
| **5** | **TaNfl1-2B** | 43014.87 | 8.96 | 49.08 | 71.17 | -0.493 | Unstable |
| **6** | **TaNOL-4D** | 37714.23 | 9.6 | 42.73 | 80.09 | -0.26 | Unstable |
| **7** | **TaNyc1-3D** | 41890.06 | 8.12 | 37.96 | 89.87 | 0.005 | Stable |
| **8** | **TaNyc3-7A** | 42721.67 | 6.02 | 54.32 | 82.27 | -0.212 | Unstable |
| **9** | **TaOsh1-4A** | 40079.08 | 6.28 | 55.69 | 74.75 | -0.579 | Unstable |
| **10** | **TaOsl2-2B** | 48653.93 | 6.81 | 42.22 | 86.15 | -0.066 | Unstable |
| **11** | **TaPME1-1B** | 58739.1 | 7.53 | 34.11 | 79.17 | 0.009 | Stable |
| **12** | **TaPNH1-7B** | 107038.12 | 9.32 | 47.07 | 81.5 | -0.387 | Unstable |
| **13** | **TaRCCR1-7D** | 35590.81 | 6.41 | 46.7 | 94.68 | 0 | Unstable |
| **14** | **TaSCR-5B** | 44271.15 | 7.82 | 67.91 | 82.17 | -0.32 | Unstable |
| **15** | **TaSGR-5D** | 31188.61 | 8.69 | 52.31 | 81.61 | -0.296 | Unstable |
| **16** | **TaSRT1-5D** | 82979.01 | 5.62 | 39.97 | 84.82 | -0.131 | Stable |
| **17** | **TaTSD2-6B** | 71552.22 | 6.61 | 40.68 | 75.09 | -0.372 | Unstable |



Table 3. Enumeration of dihedral properties of proteins after dihedral analysis through Swiss model server

| S No. | Protein | Mol Probity score | QMEAN | Stability | Solvation | Torsion | R favor (%) | State |
|---|---|---|---|---|---|---|---|---|
| **1** | **TaAct1-4B** | 0.77 | -0.48 | Stable | 0.01 | -0.41 | 97.88 | Monomer |
| **2** | **TaBri1-3D** | 1.41 | -1.97 | Stable | -2.25 | -1.35 | 92.05 | Monomer |
| **3** | **TaGATA12-3D** | 1.74 | -2.20 | Stable | 0.03 | -2.82 | 86.11 | Monomer |
| **4** | **TaNfl1-2B** | 0.87 | -1.00 | Stable | 0.60 | -1.21 | 97.52 | Monomer |
| **5** | **TaNOL-4D** | 2.66 | -4.10 | Unstable | -0.74 | -3.31 | 89.24 | Homotetramer |
| **6** | **TaNyc1-3D** | 1.53 | -3.14 | Stable | -0.84 | -2.61 | 91.88 | Homotetramer |
| **7** | **TaNyc3-7A** | 2.14 | -5.24 | Unstable | -0.41 | -4.84 | 89.47 | Monomer |
| **8** | **TaPME1-1B** | 1.43 | -2.88 | Stable | -1.32 | -2.10 | 93.71 | Monomer |
| **9** | **TaPNH1-7B** | 1.69 | -2.02 | Stable | 0.08 | -1.67 | 92.64 | Monomer |
| **10** | **TaSRT1-5D** | 1.79 | -4.55 | Unstable | -0.17 | -4.11 | 89.71 | Monomer |
| **11** | **TaOsh1-4A** | 1.28 | -0.90 | Stable | 0.61 | -1.29 | 96.67 | Monomer |
| **12** | **TaOsl2-2B** | 1.76 | -1.80 | Stable | 0.71 | -1.87 | 93.79 | Homodimer |
| **13** | **TaNAP1-7B** | 1.67 | -4.43 | Unstable | 0.26 | -3.98 | 91.18 | Monomer |
| **14** | **TaRCCR1-7D** | 1.91 | -0.28 | Stable | 0.68 | -0.29 | 94.88 | Homodimer |
| **15** | **TaSCR-5B** | 1.05 | -0.48 | Stable | 0.64 | -0.87 | 98.04 | Monomer |
| **16** | **TaSGR-5D** | 1.45 | -3.01 | Stable | -3.47 | -1.74 | 89.74 | Monomer |
| **17** | **TaTSD2-6B** | 2.41 | -3.28 | Stable | -2.04 | -2.30 | 94.7 | Monomer |



**Table 4.** Catalog of dihedral properties of candidate proteins elucidated through Ramachandran plot analysis

| S No. | Proteins | Most favored region | Generously | Additionally | Disallowed | G Score |
|---|---|---|---|---|---|---|

| | | | allowed region | allowed region | region | |
|---|---|---|---|---|---|---|
| **1.** | **TaAct1-4B** | 94.2 | 0.0 | 5.80 | 0.0 | -0.07 |
| **2.** | **TaBri1-3D** | 77.2 | 0.7 | 22.1 | 0.0 | -0.22 |
| **3.** | **TaGATA12-3D** | 75.0 | 3.6 | 21.4 | 0.0 | -0.10 |
| **4.** | **TaNAP1-7B** | 89.1 | 1.1 | 9.10 | 0.7 | -0.15 |
| **5.** | **TaNfl1-2B** | 95.2 | 1.4 | 3.40 | 0.0 | 0.07 |
| **6.** | **TaNOL-4D** | 89.2 | 1.6 | 9.00 | 0.6 | -0.20 |
| **7.** | **TaNyc1-3D** | 88.1 | 0.7 | 10.6 | 0.6 | -0.13 |
| **8.** | **TaNyc3-7A** | 86.1 | 0.5 | 12.5 | 1.0 | -0.32 |
| **9.** | **TaOsh1-4A** | 96.3 | 0.0 | 3.70 | 0.0 | -0.07 |
| **10.** | **TaOsl2-2B** | 87.8 | 0.8 | 10.8 | 0.6 | -0.12 |
| **11.** | **TaPME1-1B** | 87.1 | 0.4 | 12.5 | 0.0 | -0.16 |
| **12.** | **TaPNH1-7B** | 88.9 | 1.4 | 9.40 | 0.3 | -0.09 |
| **13.** | **TaRCCR1-7D** | 90.2 | 0.0 | 9.60 | 0.2 | -0.14 |
| **14.** | **TaSCR-5B** | 95.6 | 0.0 | 4.40 | 0.0 | 0.02 |
| **15.** | **TaSGR-5D** | 82.4 | 0.0 | 14.7 | 2.9 | -0.15 |
| **16.** | **TaSRT1-5D** | 86.5 | 1.9 | 11.0 | 0.6 | -0.23 |
| **17.** | **TaTSD2-6B** | 88.8 | 1.7 | 8.60 | 0.9 | -0.28 |

1067

Figure 1.TIFF

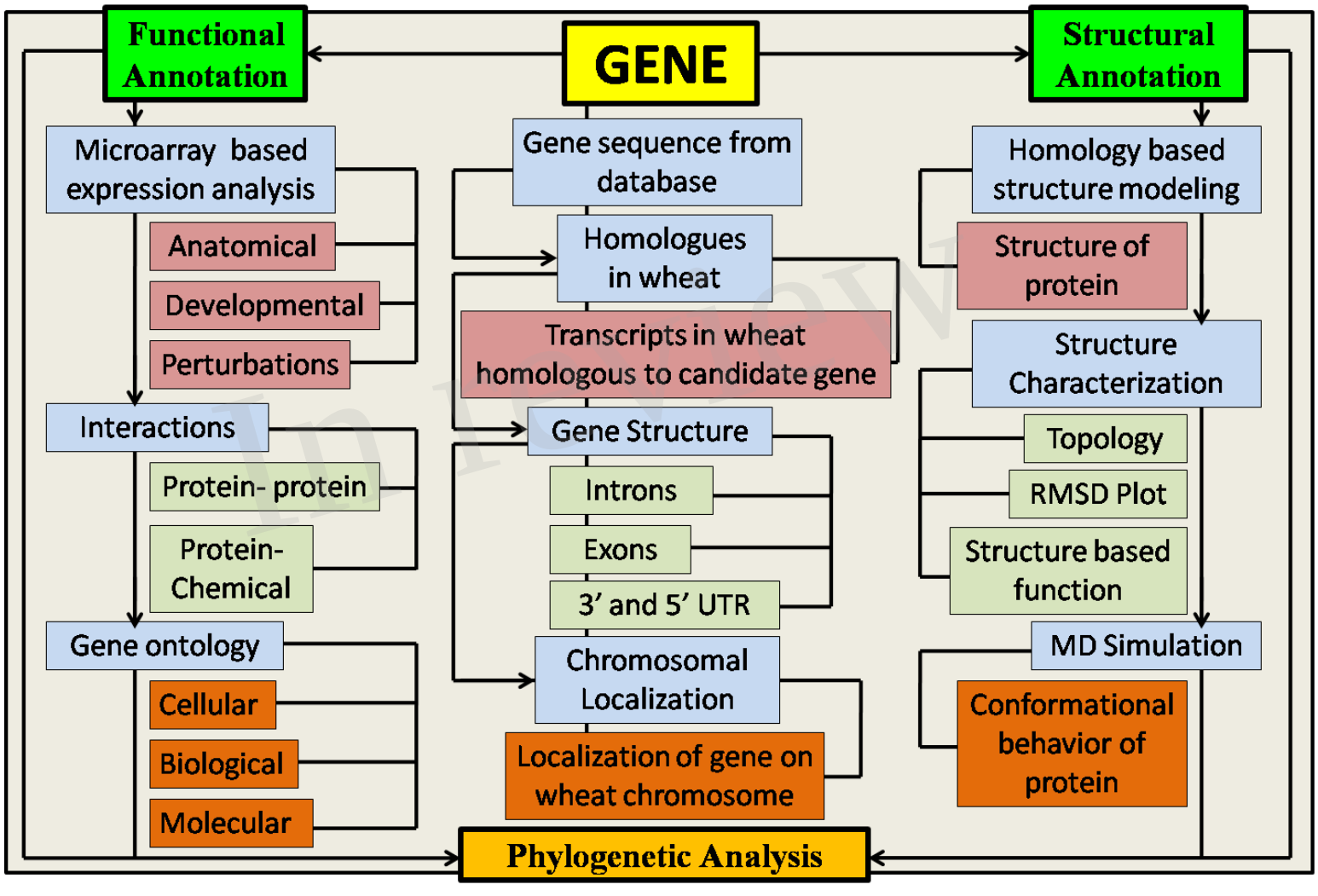

Figure 2.TIFF



Figure 3.TIFF

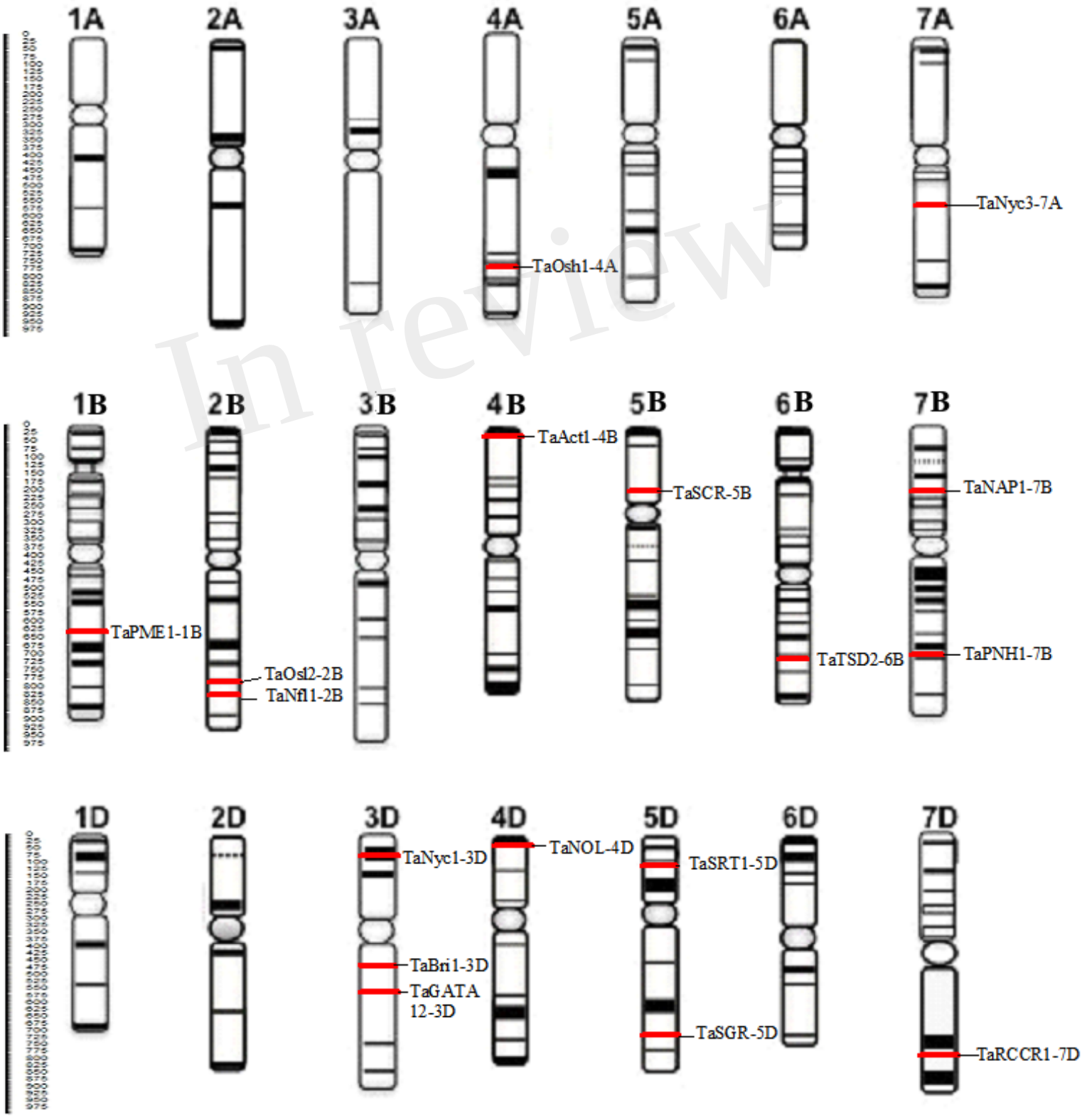

Figure 4.TIFF

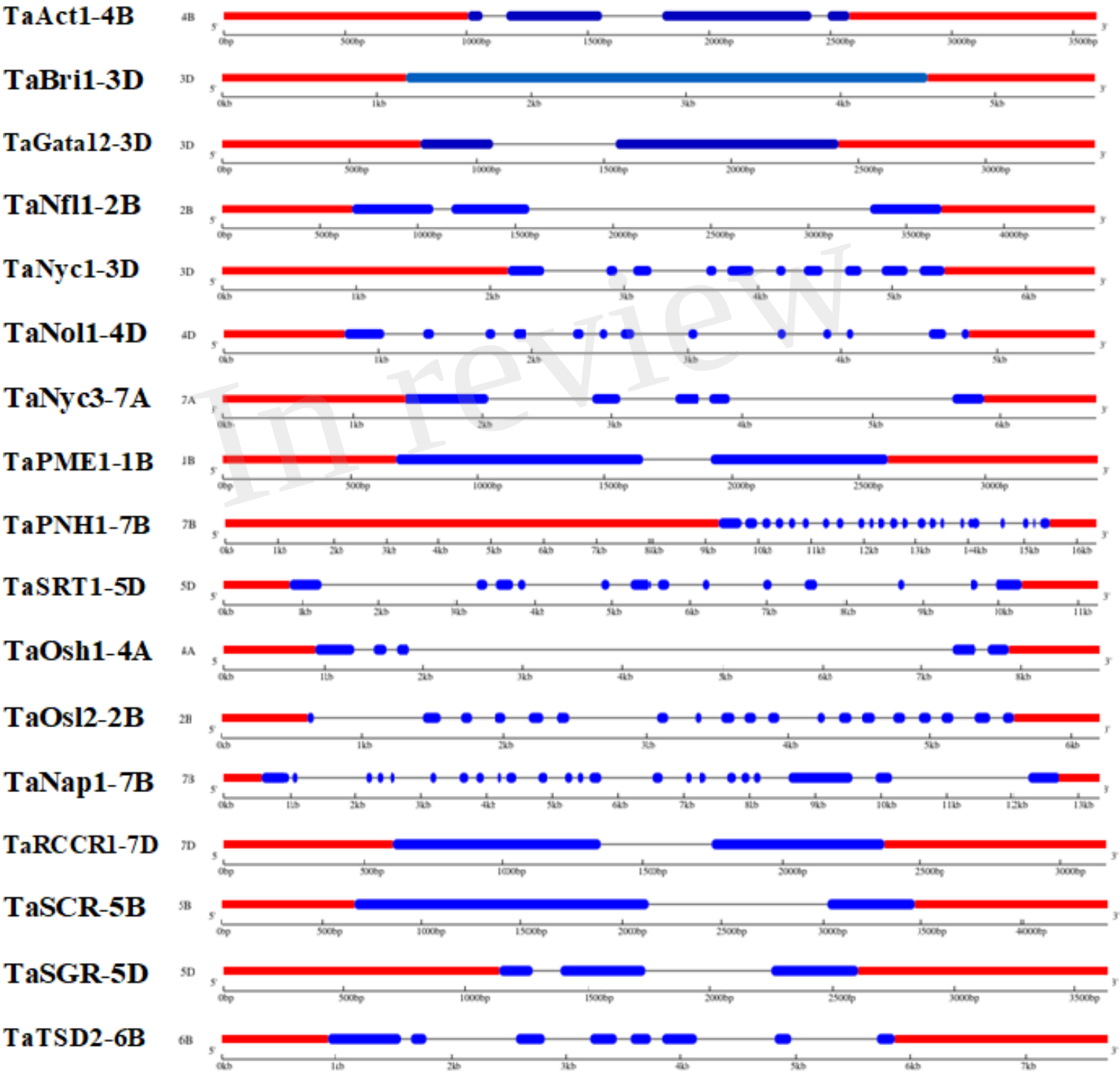

Figure 5.TIFF

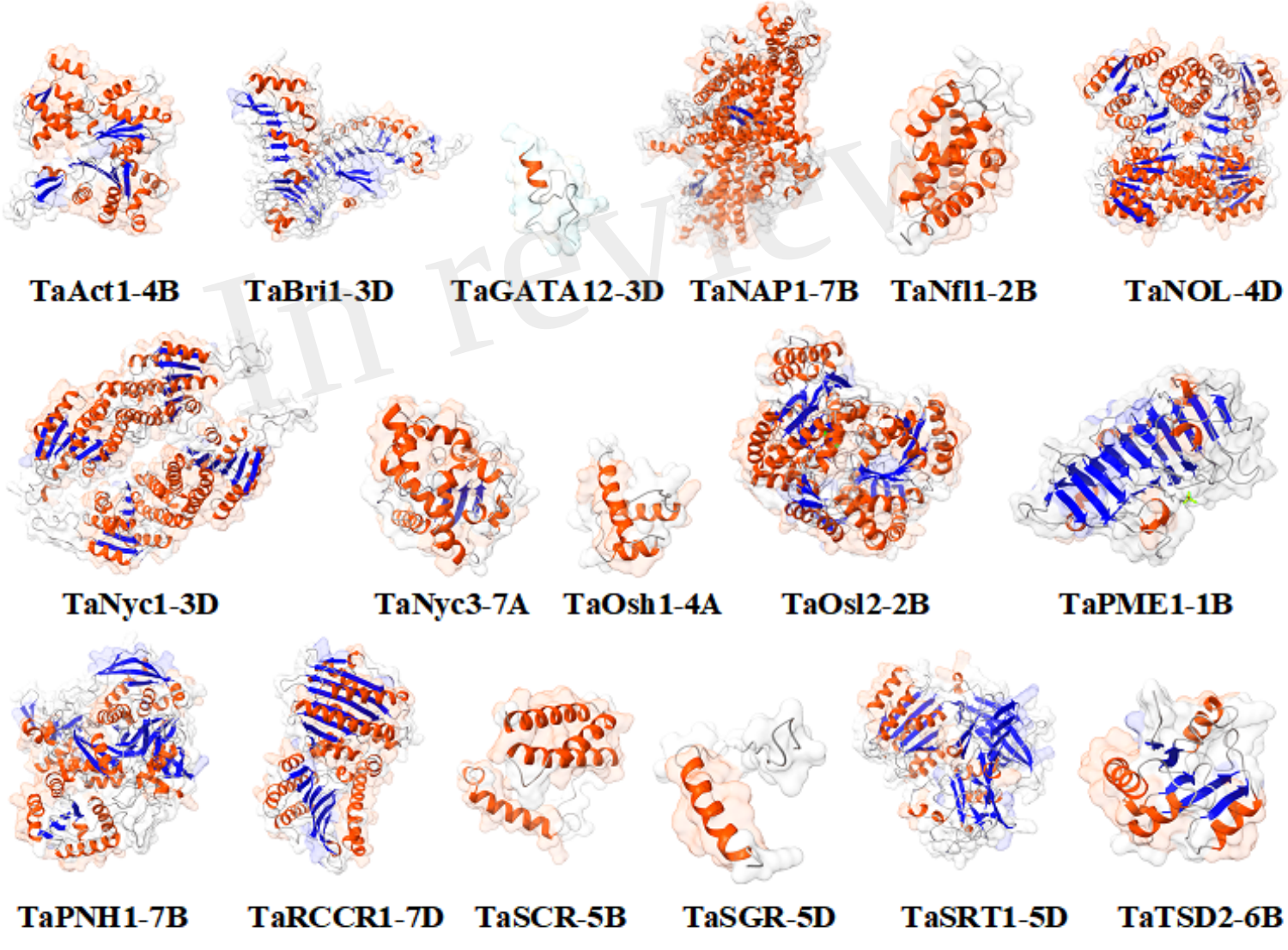

Figure 6.TIFF

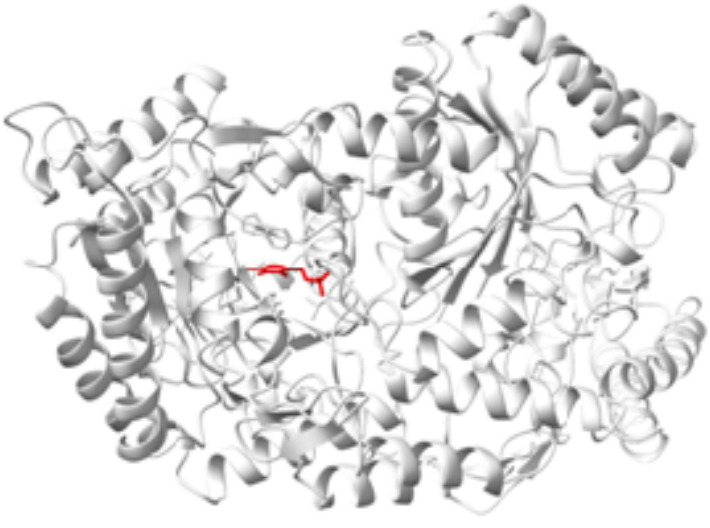

TaOsl2-2B

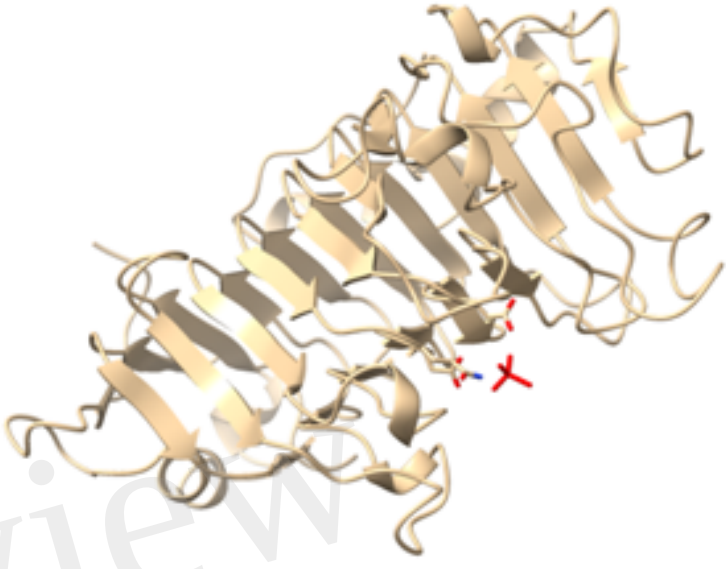

TaPME1-1B

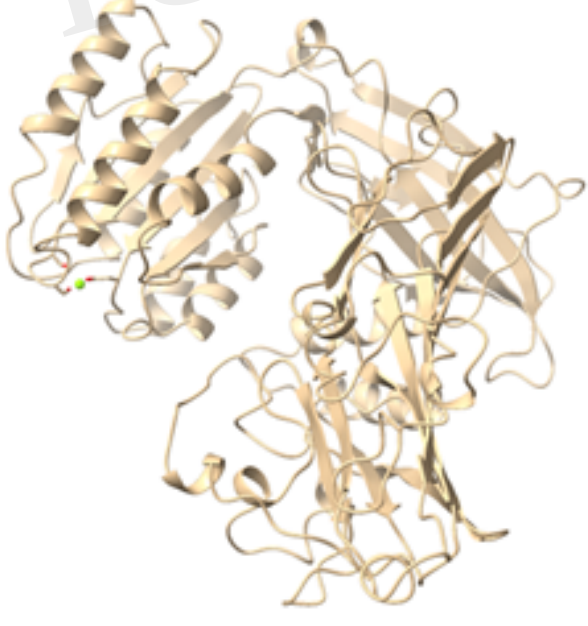

TaSRT1-5D

Figure 7.TIFF

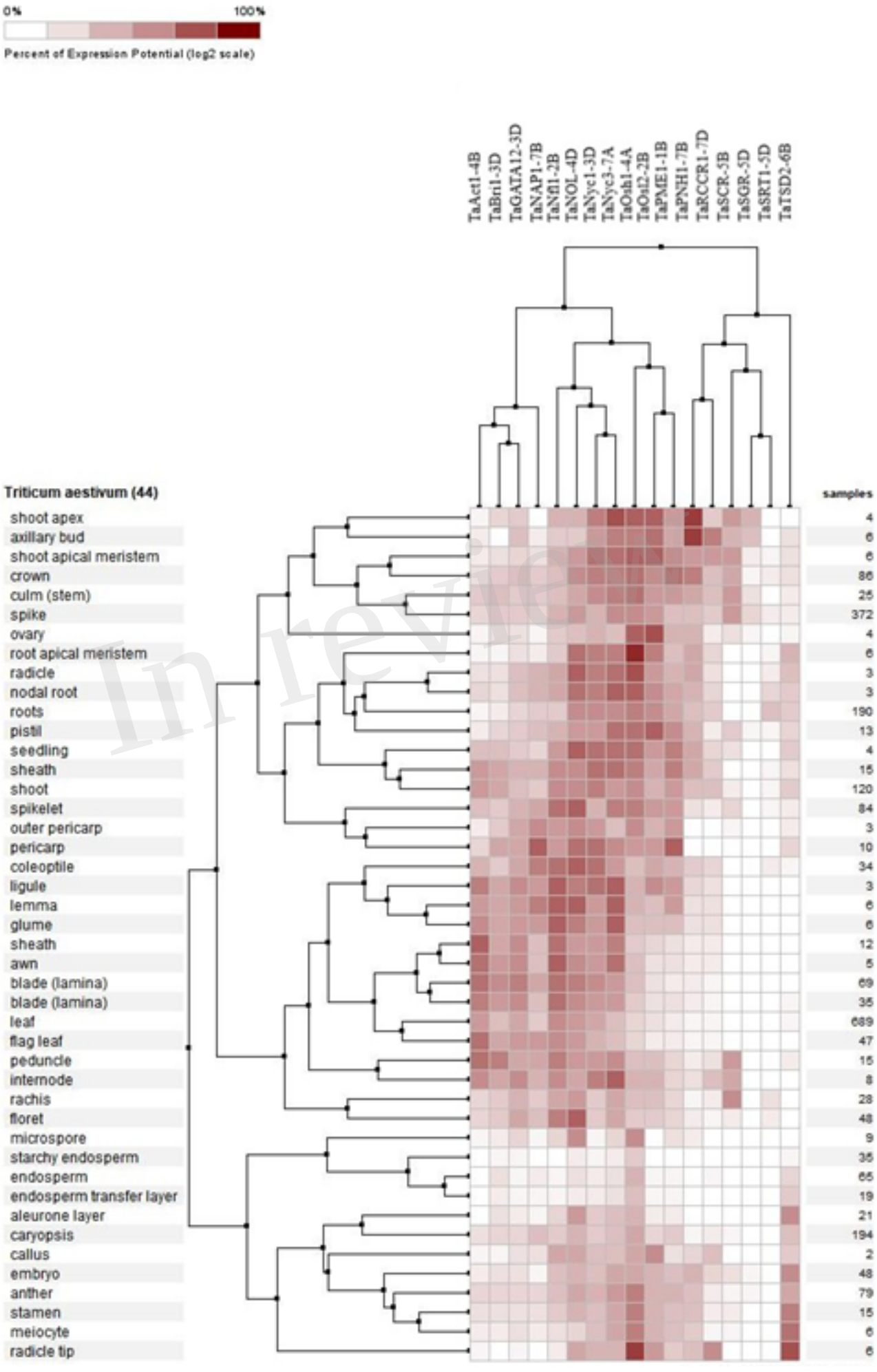

Figure 8.TIFF

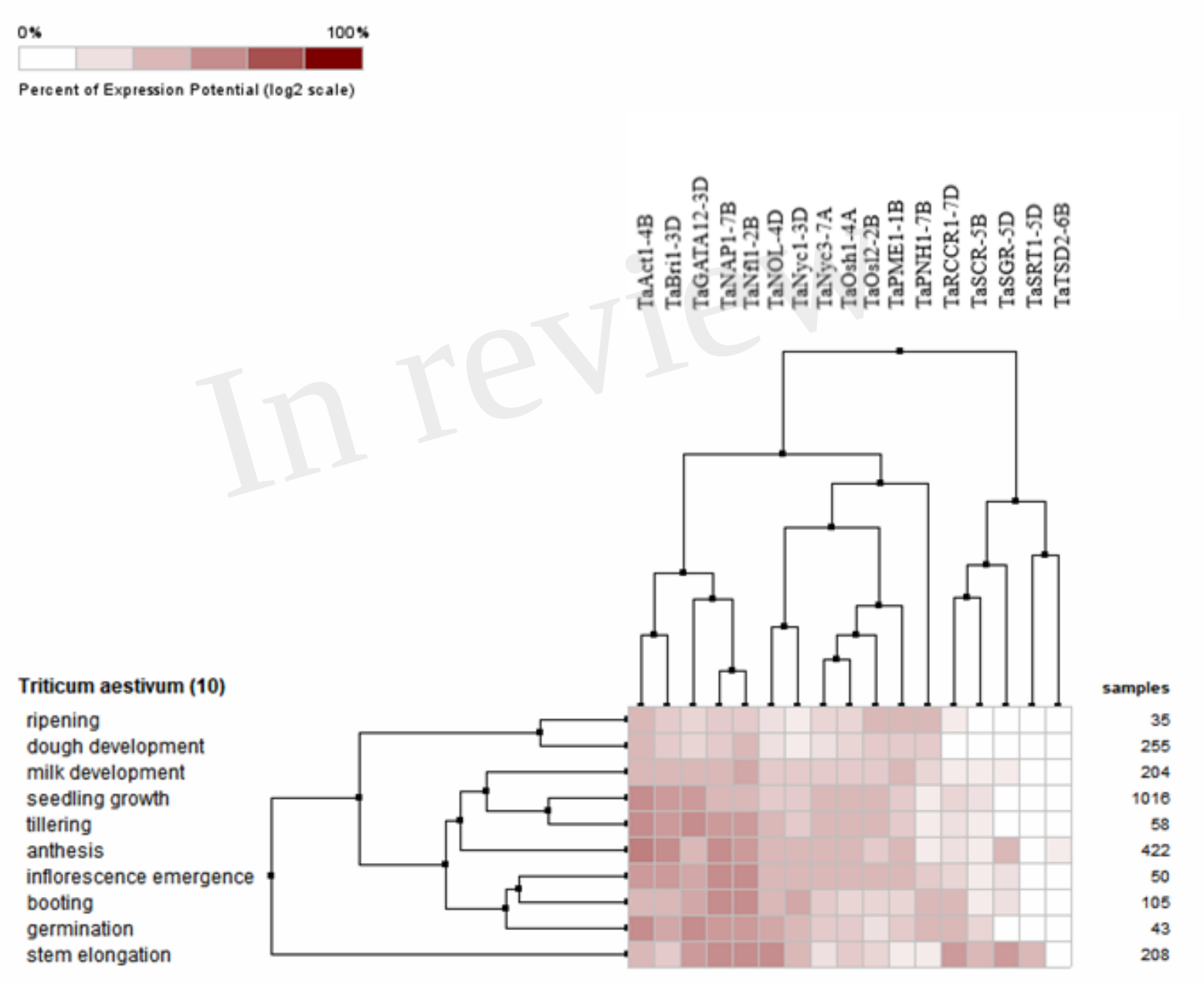

Figure 9.TIFF

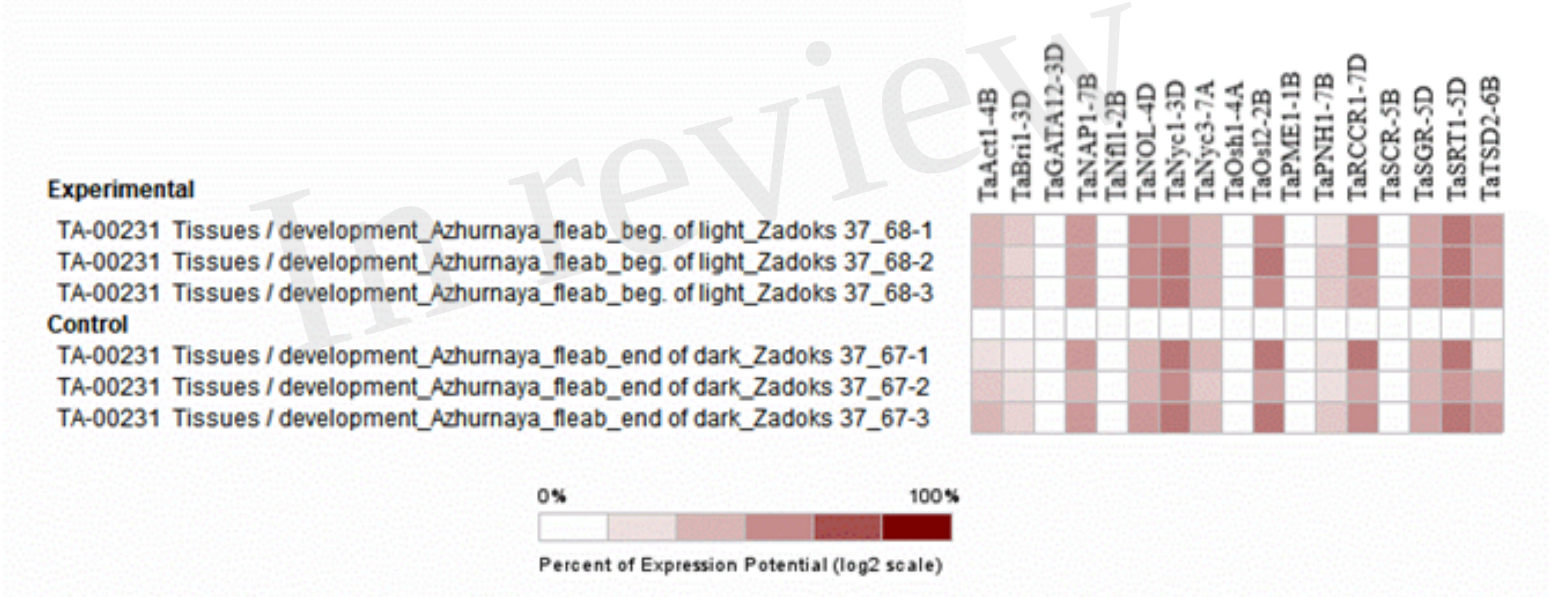

Figure 10.TIFF

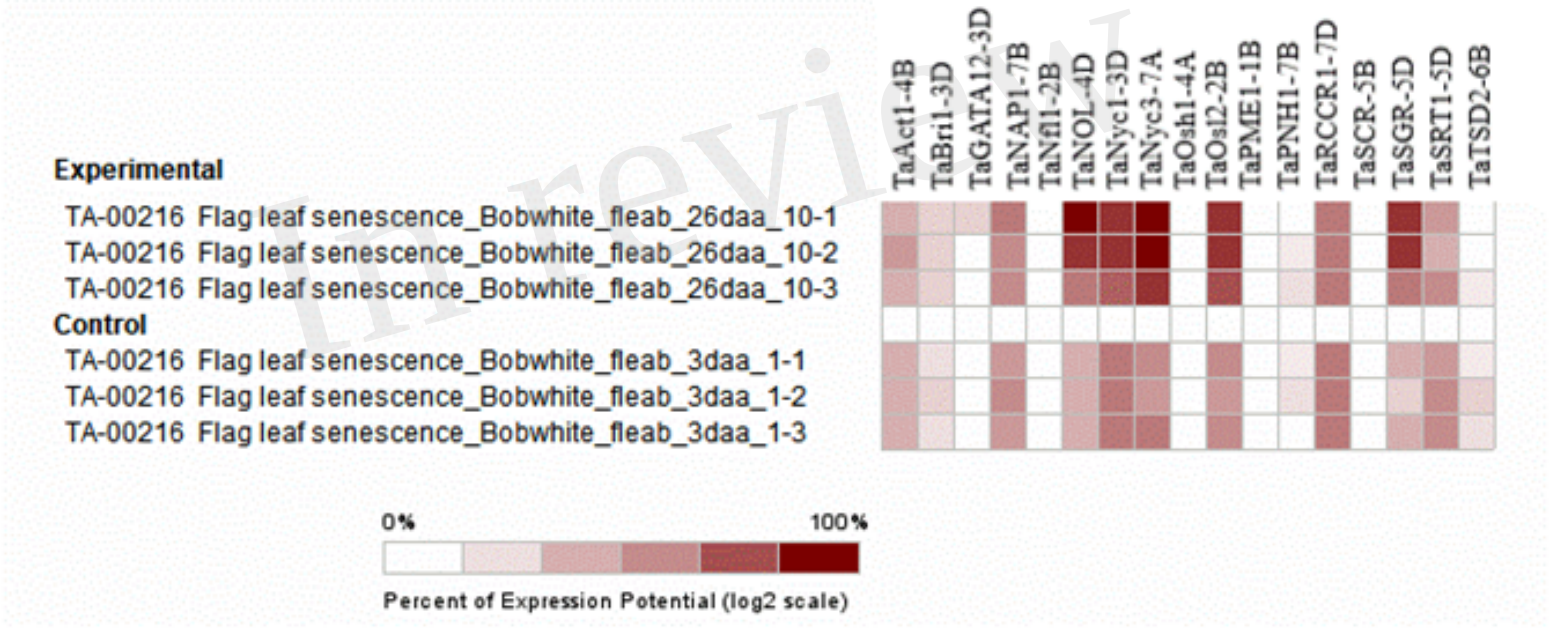

Figure 11.TIFF

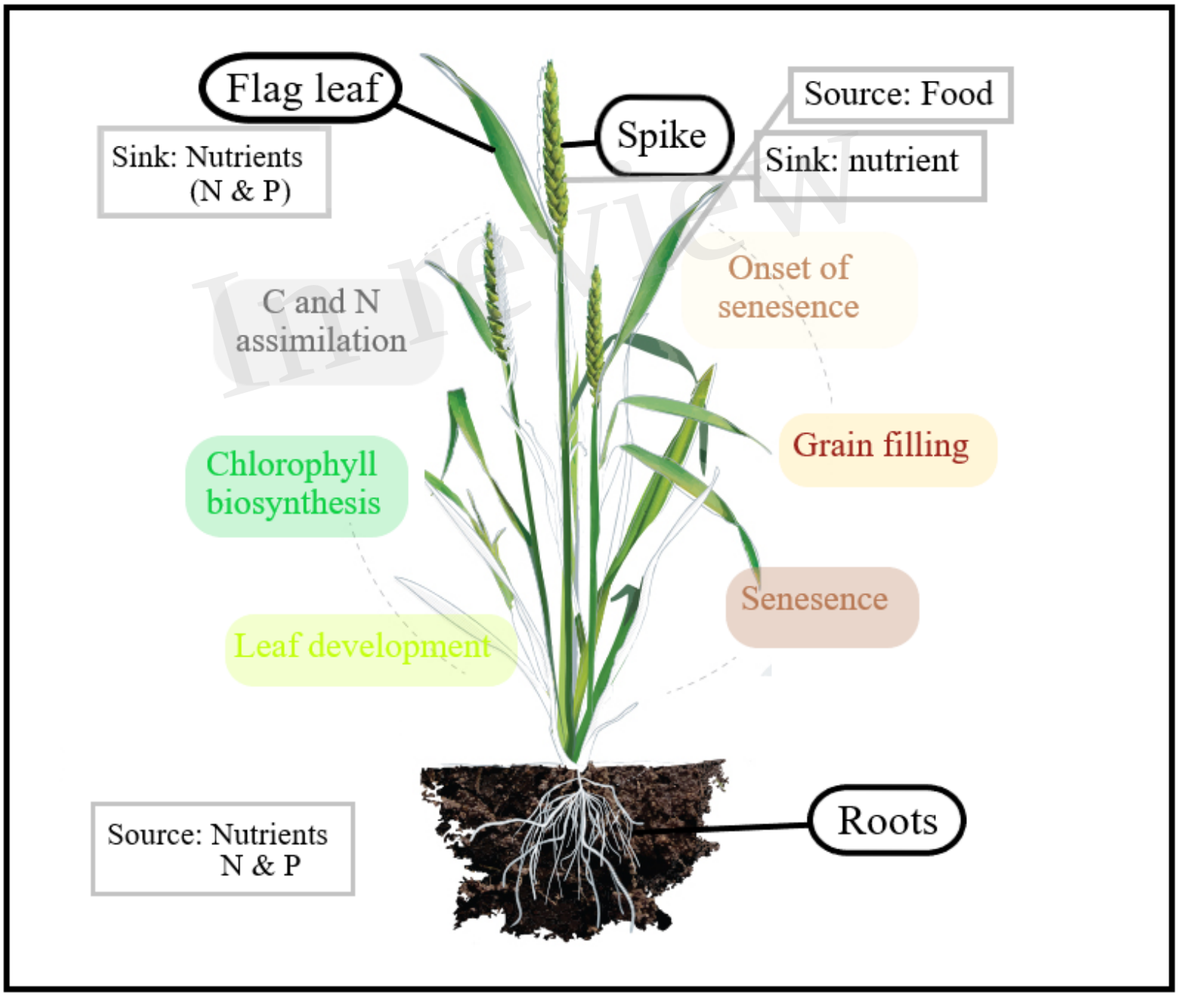

Figure 12.TIFF

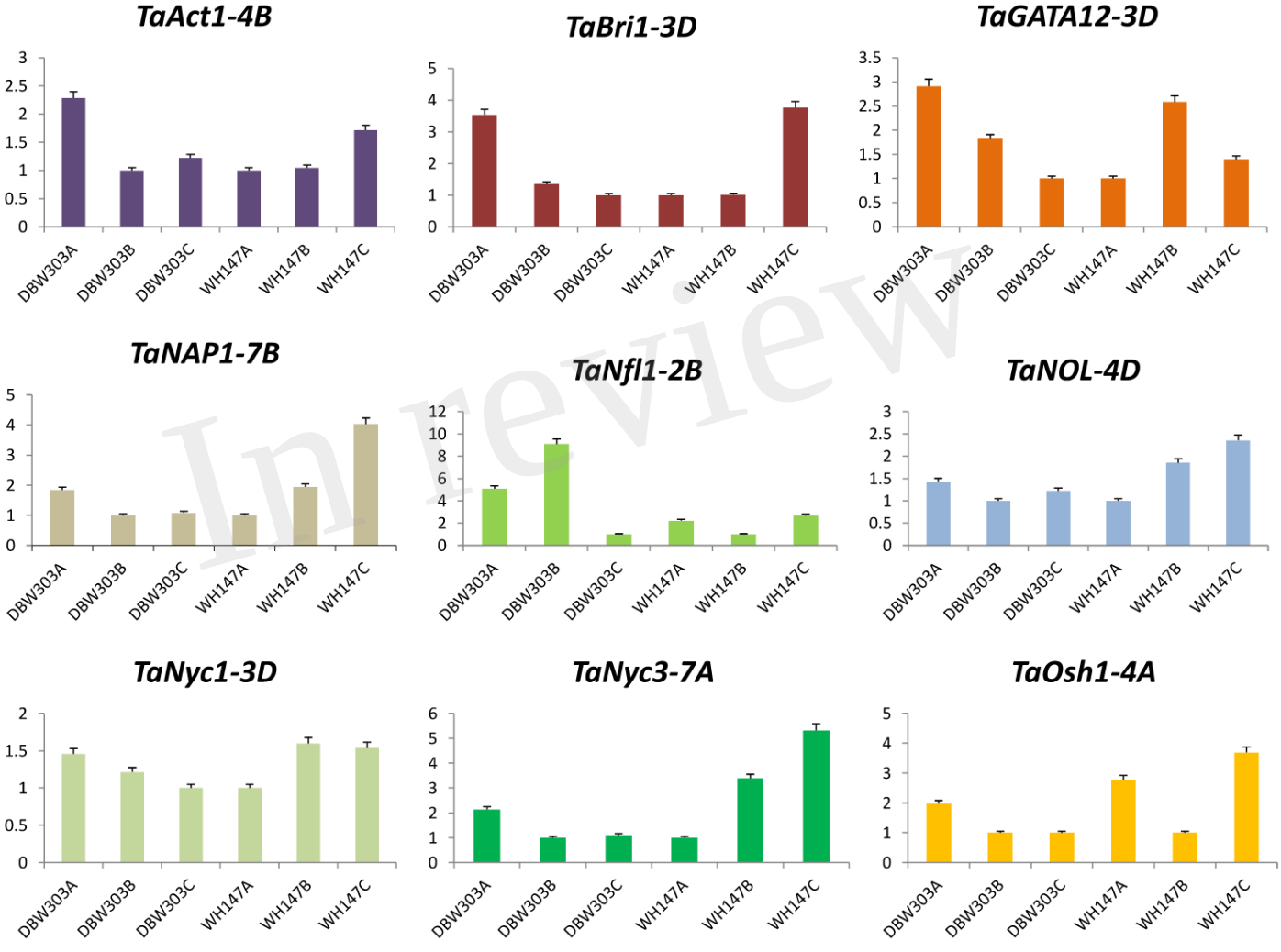

Figure 13.TIFF

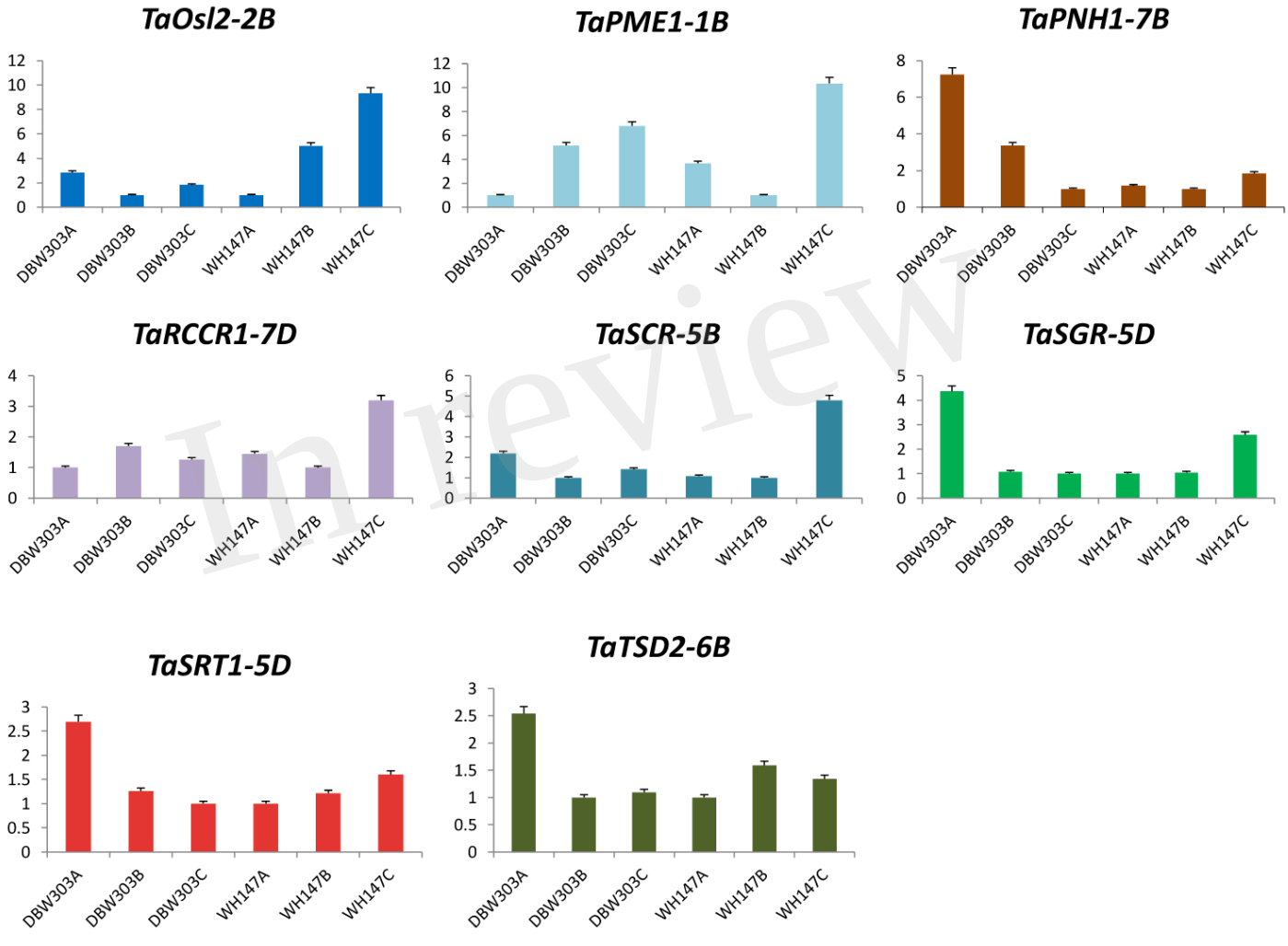

Figure 14.TIFF

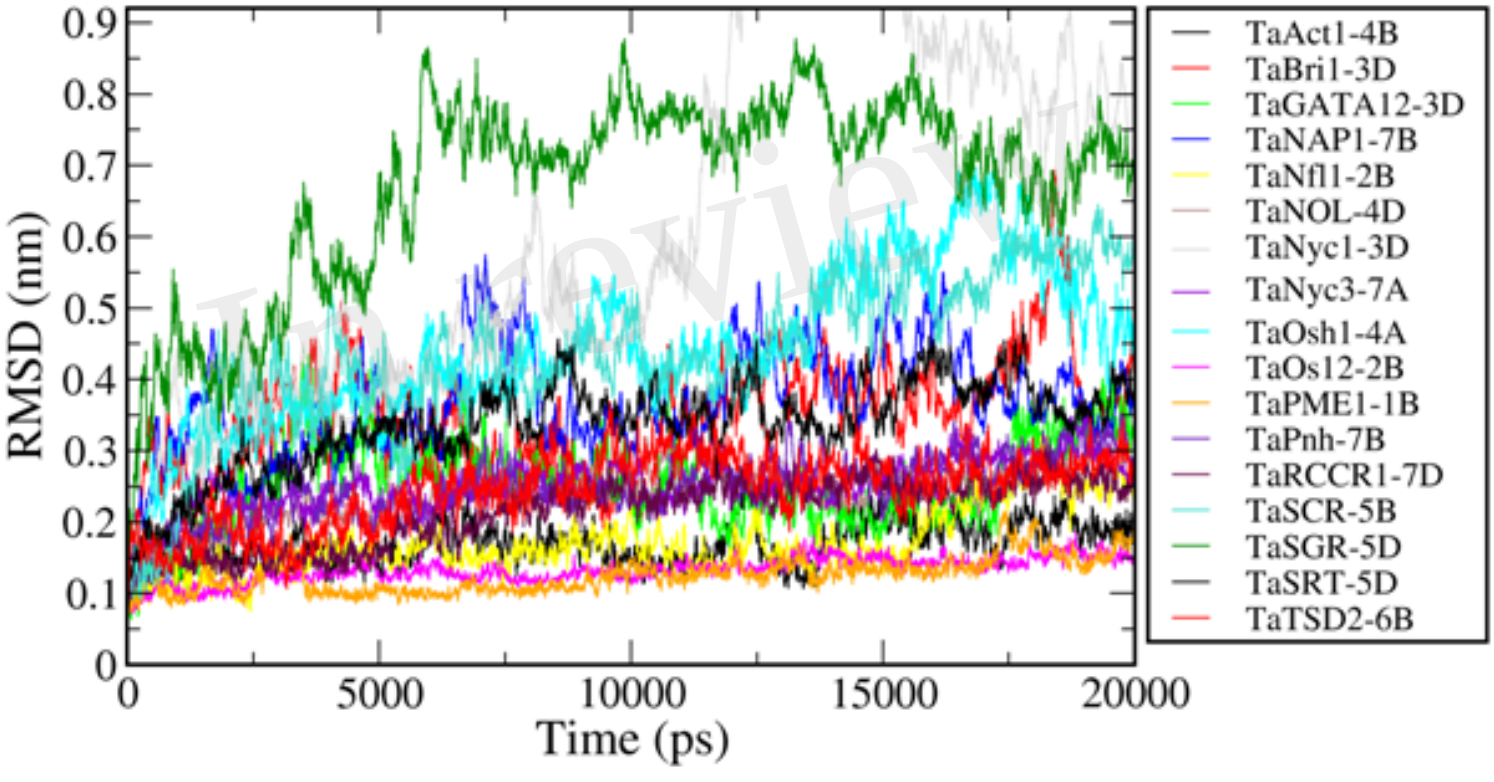

Figure 15.TIFF